# Anomalous quadrupole collectivity of neutron-rich Mg isotopes near the drip line

**K. Yoshida (Kyoto U.)**

based on KY, arXiv:2109.08328

# Strong quadrupole deformation beyond *N*=20

✓ breaking of the spherical *N*=20 magic number at $^{32}$Mg

low $E(2_1^+)$ and high $B(\mathrm{E2})$

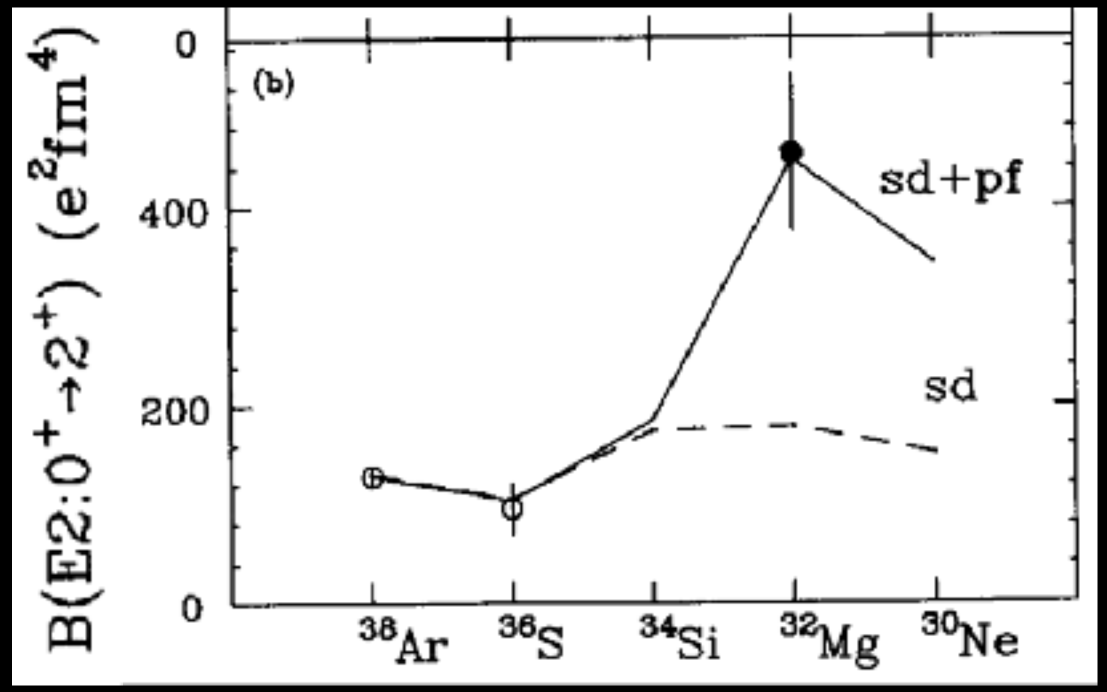


Motobayashi+, PLB346(1995)9

✓ “stable” quadrupole deformation beyond *N*=20

Doornenbal+, PRL111(2013)212502

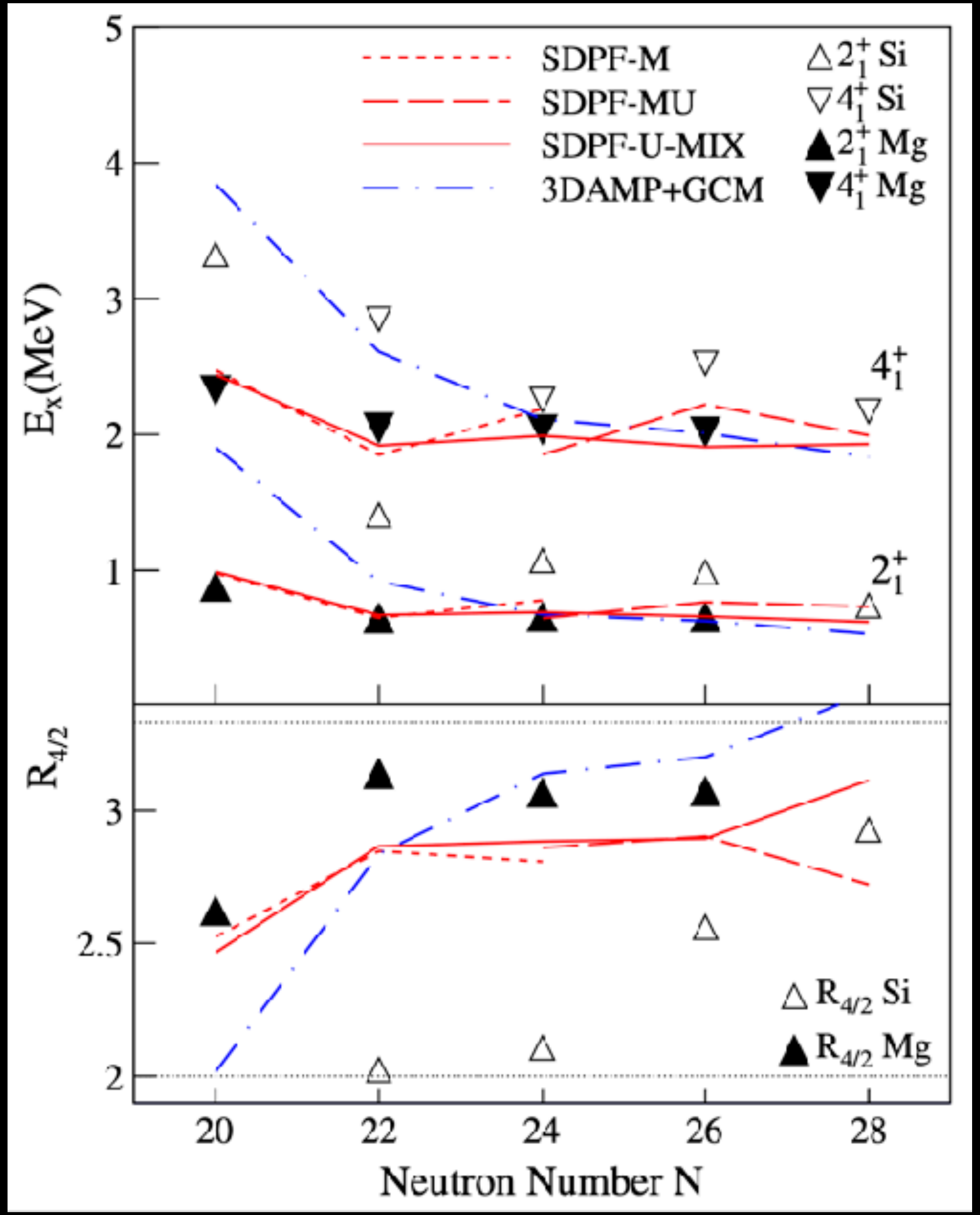


Crawford+, PRL122(2019)052501

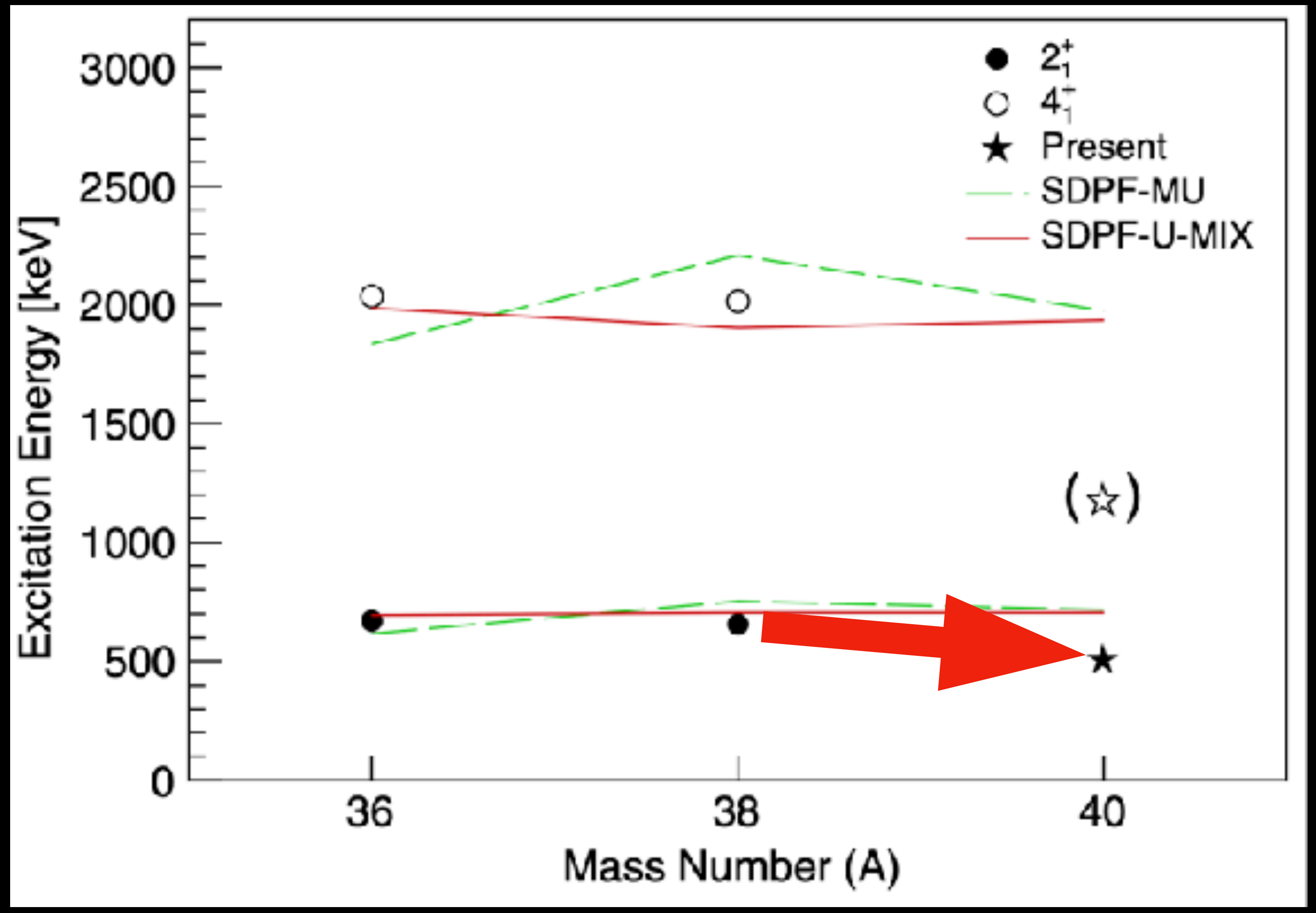


635(6) keV →500(14) keV

~20% decrease in energy

# Why so low at $^{40}$Mg?

Rodríguez, EPJA52(2016)190

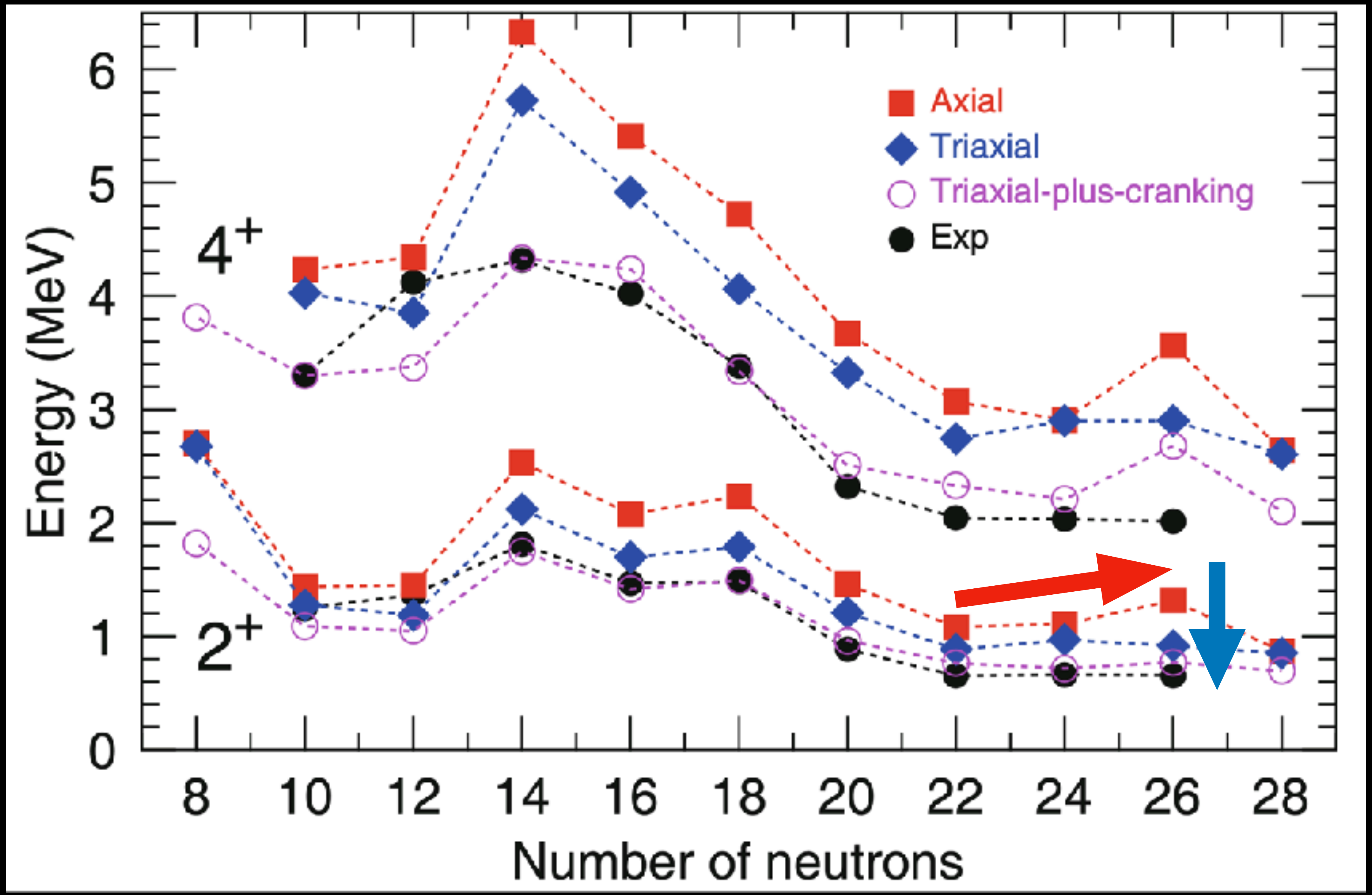


Shimada+, PRC93(2016)064314 BMF: beyond mean-field

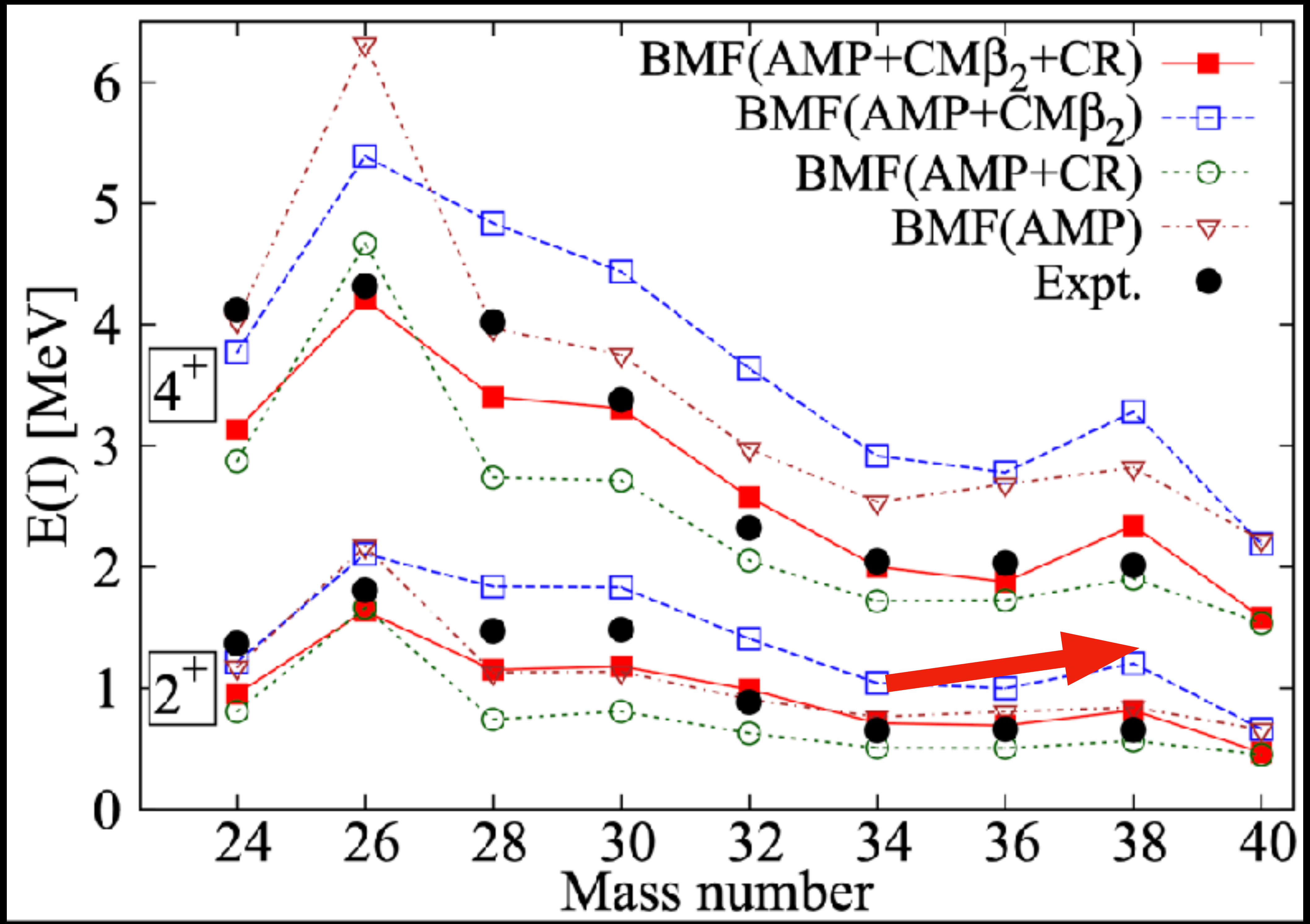


β-GCM: upward trend toward *N*=26 and decrease at *N*=28

βγ-GCM: triaxial dynamics lowers $E(2^+)$ at *N*=26

cf. important roles of triaxiality at *N*=26

Suzuki–Kimura, PRC104(2021)024327

weak binding/continuum effects?

# Simple mean-field analysis within DFT

not easy to incorporate the continuum effects into the BMF model

coordinate-space Hartree–Fock–Bogoliubov formalism

Dobaczewski–Flocard–Treiner, NPA422(1984)103

↓

cranking for non-zero spins $\delta(E[\rho] - \omega_{\rm rot}\langle \hat{J}_z \rangle) = 0$

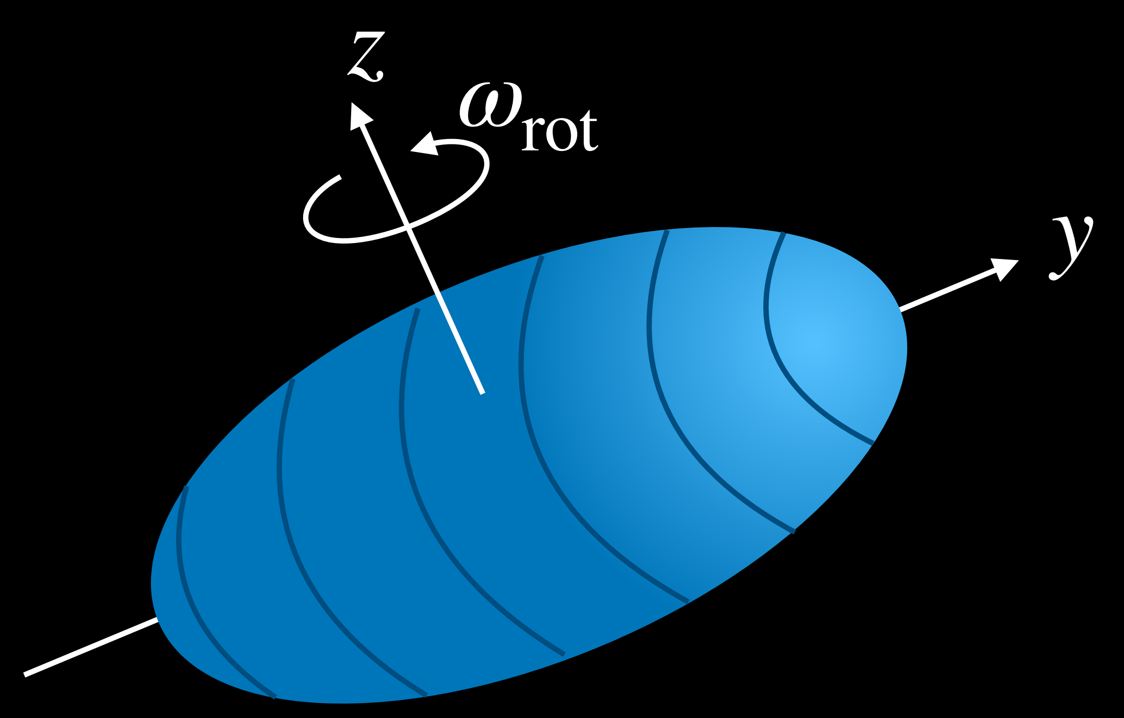


standard technique for solving the cranked-HFB (3D-HFB) eq.

two-basis method

Gall+, ZPA348(1994)183

Terasaki+, NPA621(1997)706

Hartree–Fock $\{\phi_i\}$ → HFB in a truncated space

non-localized single-particle states in the continuum enter the pairing window

one needs to enlarge the truncated space

full diagonalization of the HFB Hamiltonian possible using modern computers

**parallel solver for the HFB eq. in the 3D-Cartesian-mesh** KY, arXiv:2109.08328

# 3D-coordinate-space (Cartesian-mesh) representation

sp wavefunctions

$$\varphi_{\vec{n}} \equiv \varphi(\vec{r} = \Delta L \vec{n})$$

$$\vec{n} = (n_x, n_y, n_z)$$

$$(n_x, n_y, n_z) = 0, \pm 1, \cdots \pm M$$

advantage

- exotic deformation
- weakly-bound nuclei
- simple coding

1/8 reduction

P. Bonche et al., NPA443(1985)39

$$\varphi_{\vec{n}} \equiv \varphi(\vec{r} = \Delta L \vec{n})$$

$$\vec{n} = (n_x, n_y, n_z)$$

$$(n_x, n_y, n_z) = 0, 1, \cdots M$$

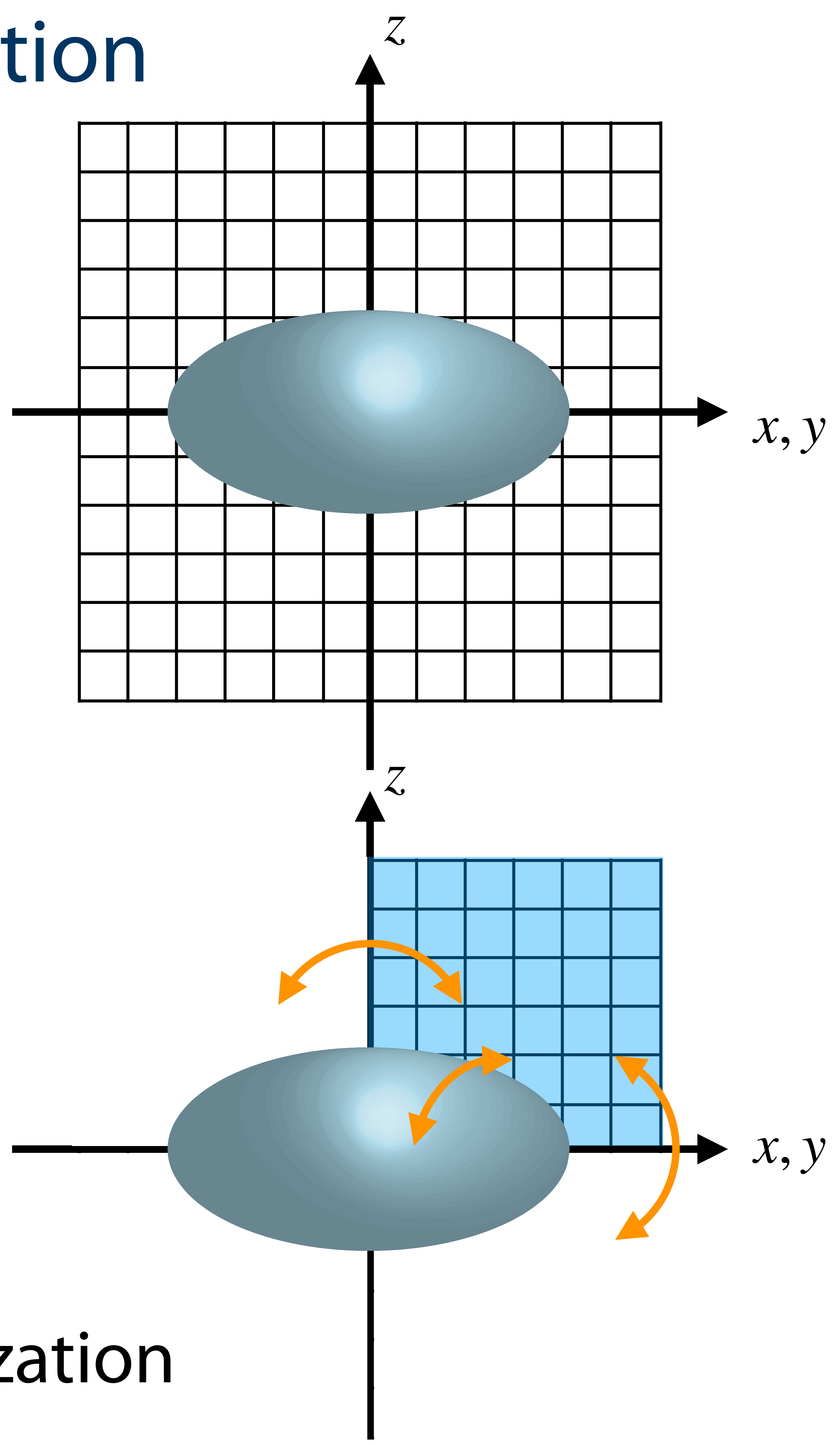


In the present calculation,

$\Delta L = 1.0$ fm $\quad \dim(H) = 8M^3 = 13824 @ M = 12$

direct diagonalization

parallelization in parity, z-signature, neutrons/protons, spatial grid

# Density-dependence of the pairing int.

moments of inertia ⟷ superfluidity

Mixed-type: $V_0 = -295$ MeV fm³ according to KY, EPJA42(2009)583

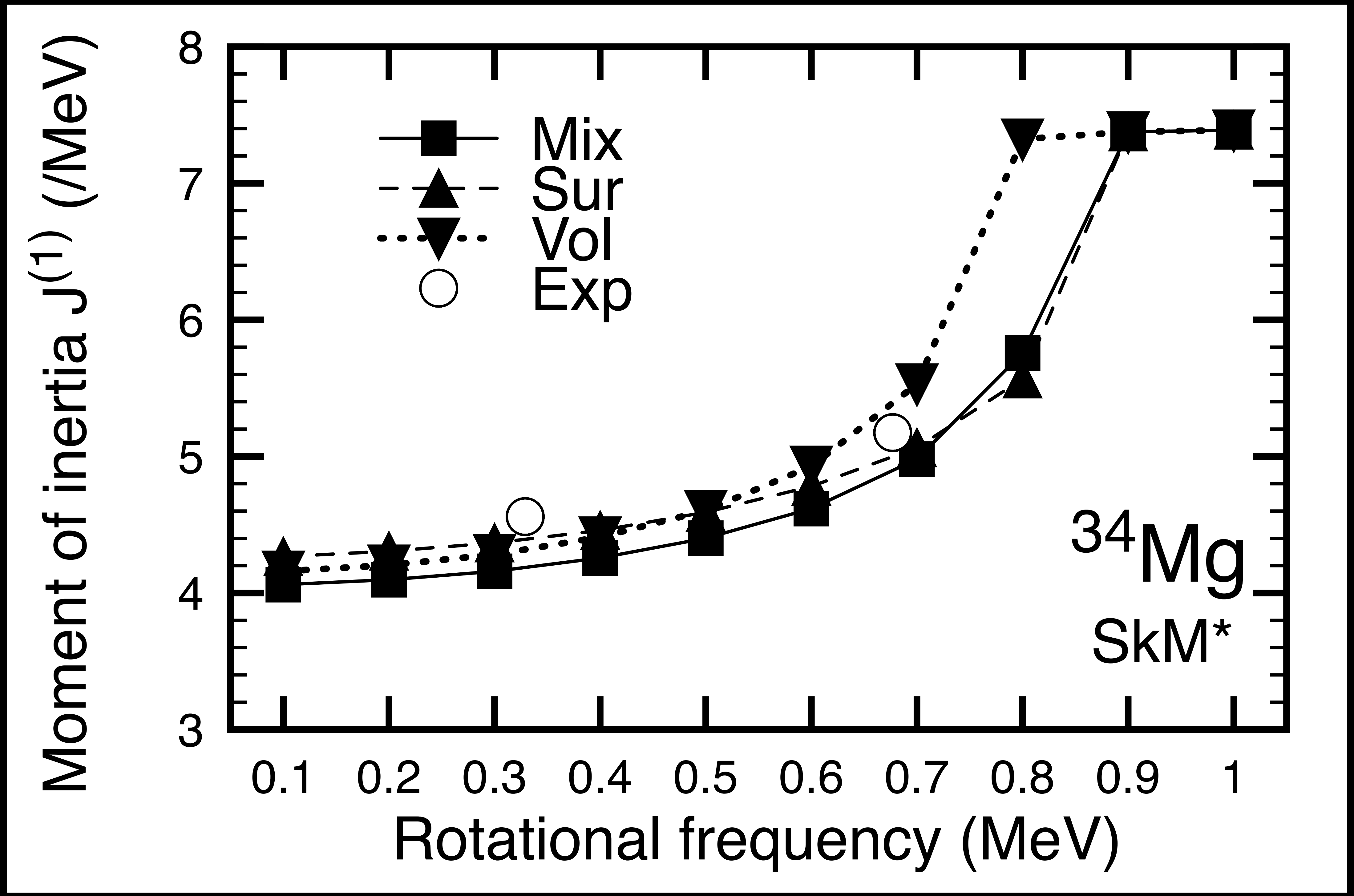


Exp: Michimasa+, PRC89(2014)054307

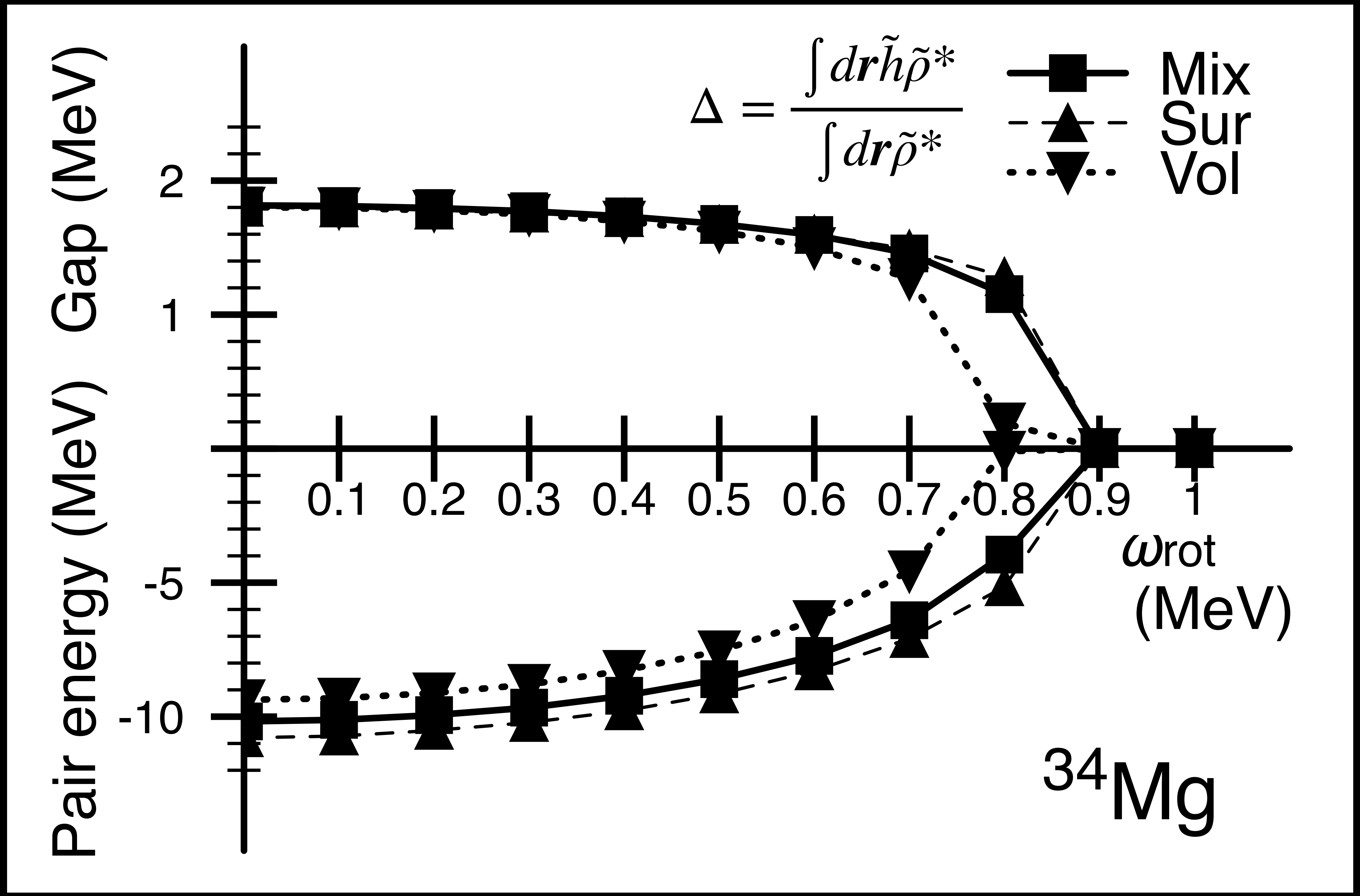


volume pairing: slightly weak correlation

low-spin states are well described

not very sensitive to the density dependence

# Isotopic dependence of the low-spin yrast states

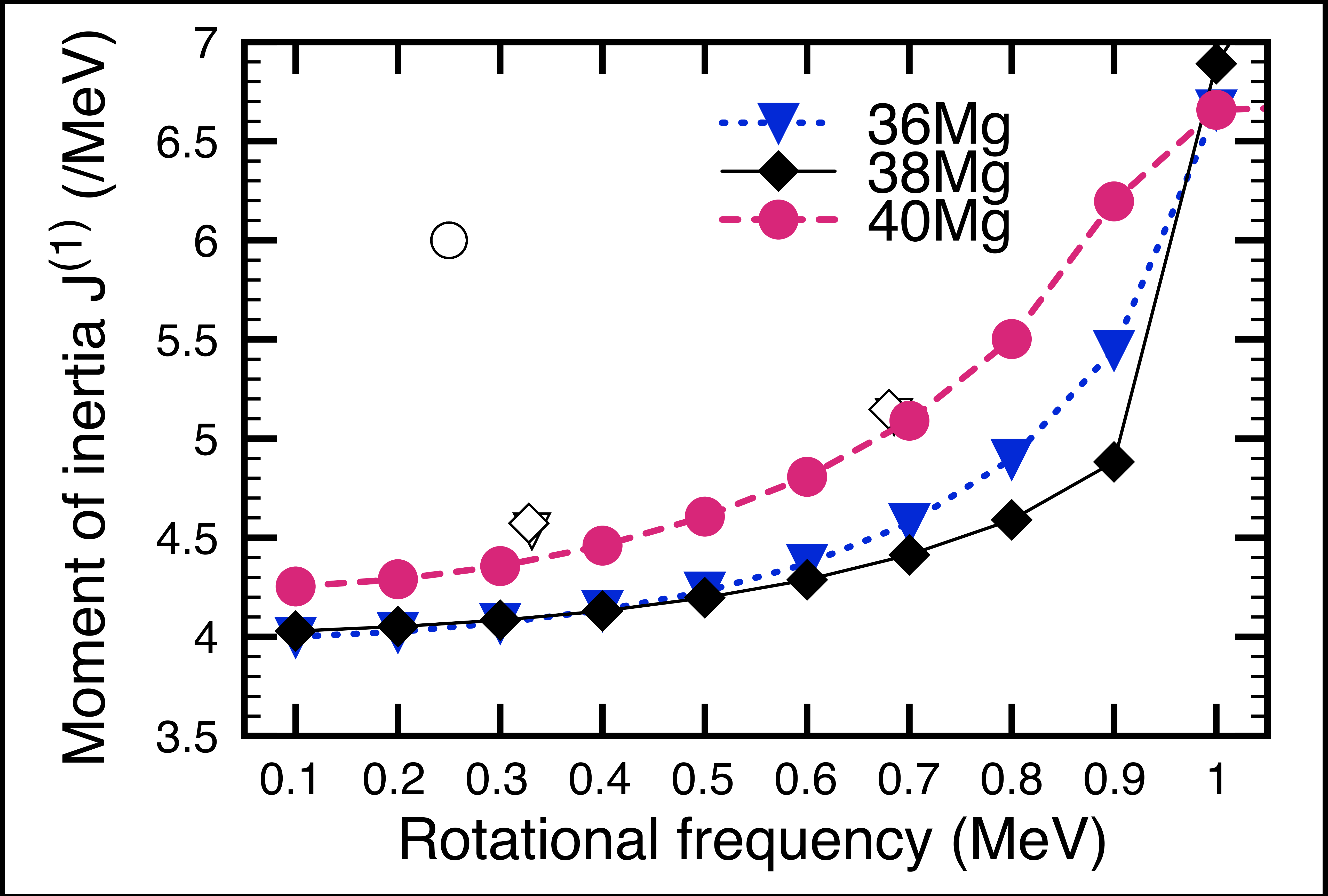


Exp: Doornenbal+, PRL111(2013)212502
Crawford+, PRL122(2019)052501

$^{36,38}$Mg

slight underestimation of $\mathscr{J}^{(1)}$

$^{40}$Mg

$\mathscr{J}^{(1)}$(cal) far below the observed one
overestimation of $E(2^+)$

the present model does not explain the observed isotopic dep.

# Anomaly in $^{40}$Mg

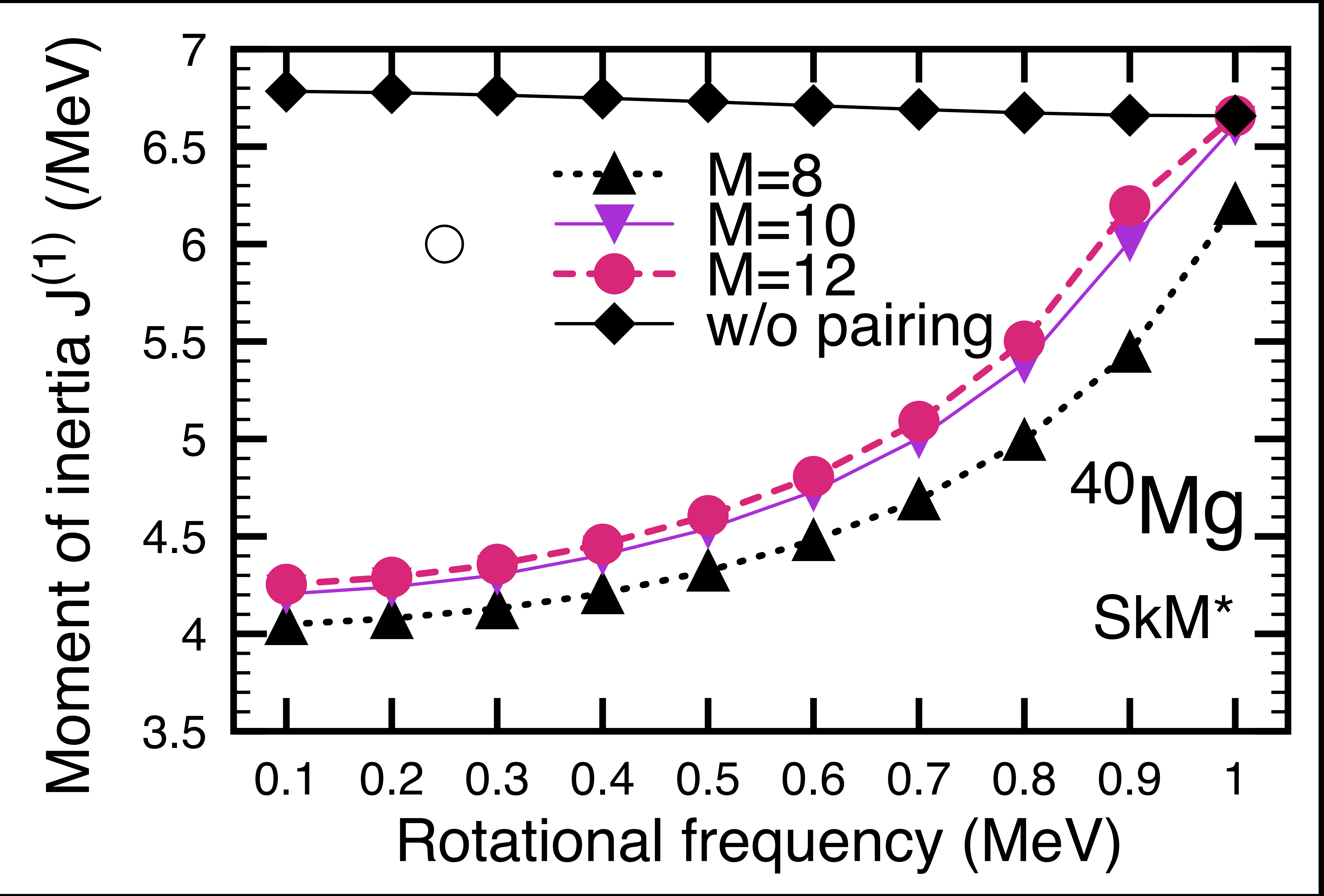


$\mathscr{J}^{(1)} \uparrow$ with an increase in the box size

convergence with $M = 10 - 12$

oblate config. $\mathscr{J}^{(1)} = 1.9$ MeV$^{-1}$

weak-binding effect does not explain the obs.

pairing plays a more important role

# Pairing functional considering the neutron-excess effect

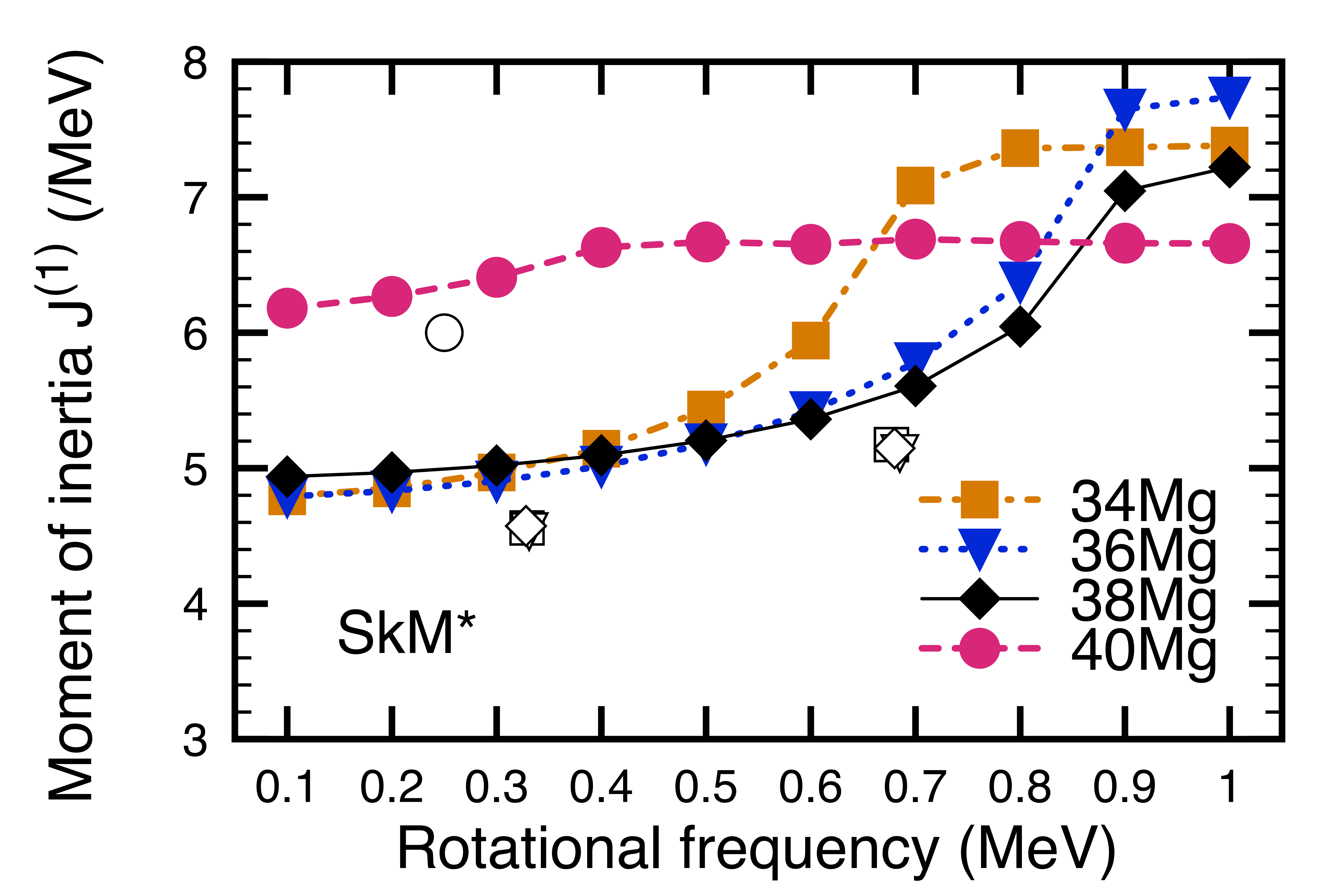


Yamagami–Shimizu–Nakatsukasa, PRC80(2009)064301

$$H(\boldsymbol{r}) = \frac{V_0}{4} \sum_{\tau=n,p} g_\tau[\rho, \rho_1] \, |\tilde{\rho}_\tau(\boldsymbol{r})|^2$$

$$g_\tau[\rho, \rho_1] = 1 - \eta_0 \frac{\rho_0(\boldsymbol{r})}{\rho_{\rm nn}} - \eta_1 \frac{\tau_3 \rho_1(\boldsymbol{r})}{\rho_{\rm nn}} - \eta_2 \left( \frac{\rho_1(\boldsymbol{r})}{\rho_{\rm nn}} \right)^2$$

weakening of pairing at $^{40}$Mg

isospin-dependence of the paring

deformed gap at $N = 28$

pairing does play an important role

low-lying states in n-rich nuclei ➡ construction of a global pairing EDF

# Weak-binding effects in low-spin states

$M = 14$

$\dim(H) = 8M^3 = 21952$

$J_z^2 = I(I+1)$

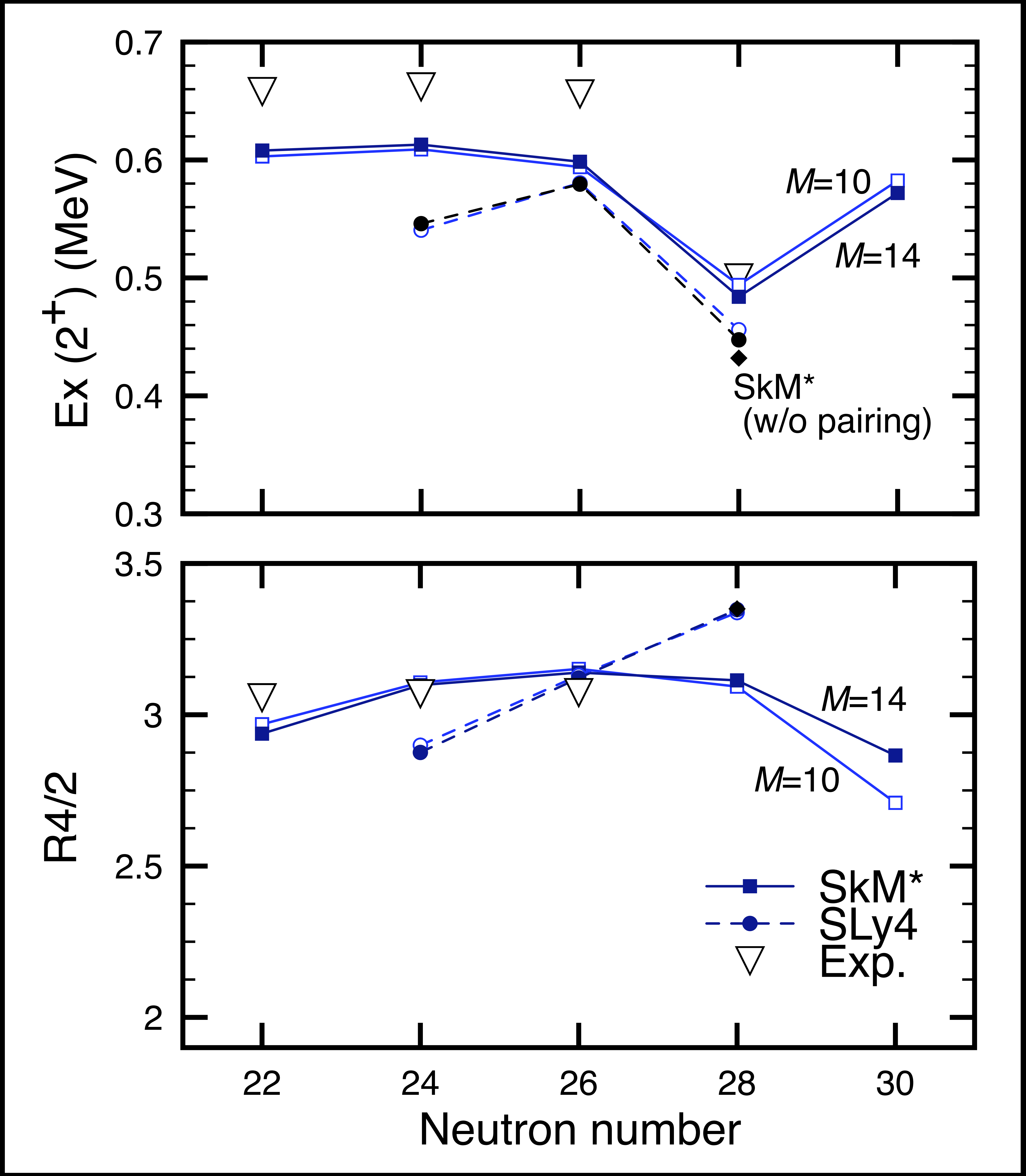


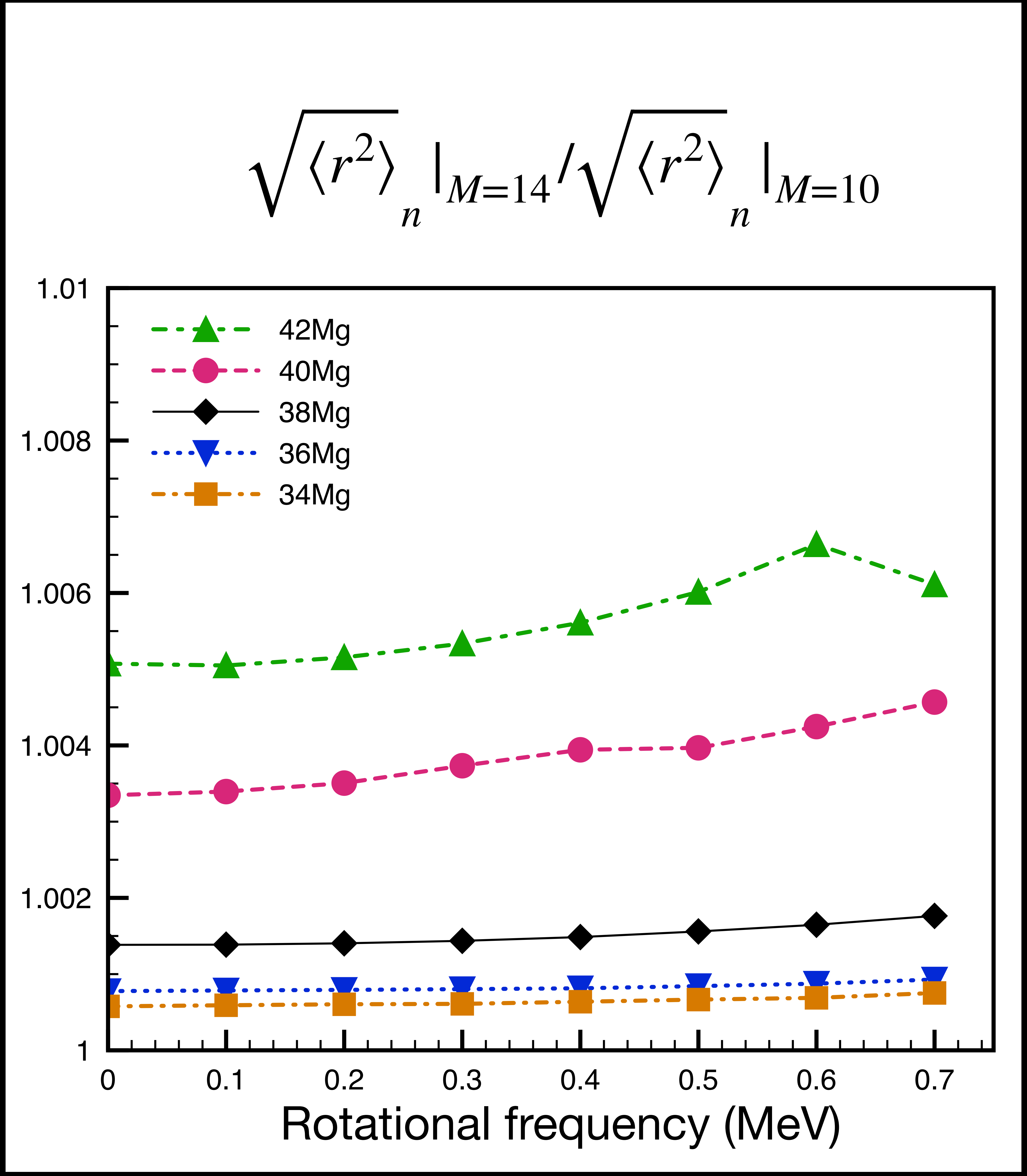

# Functional dependence

$J_z^2 = I(I+1)$

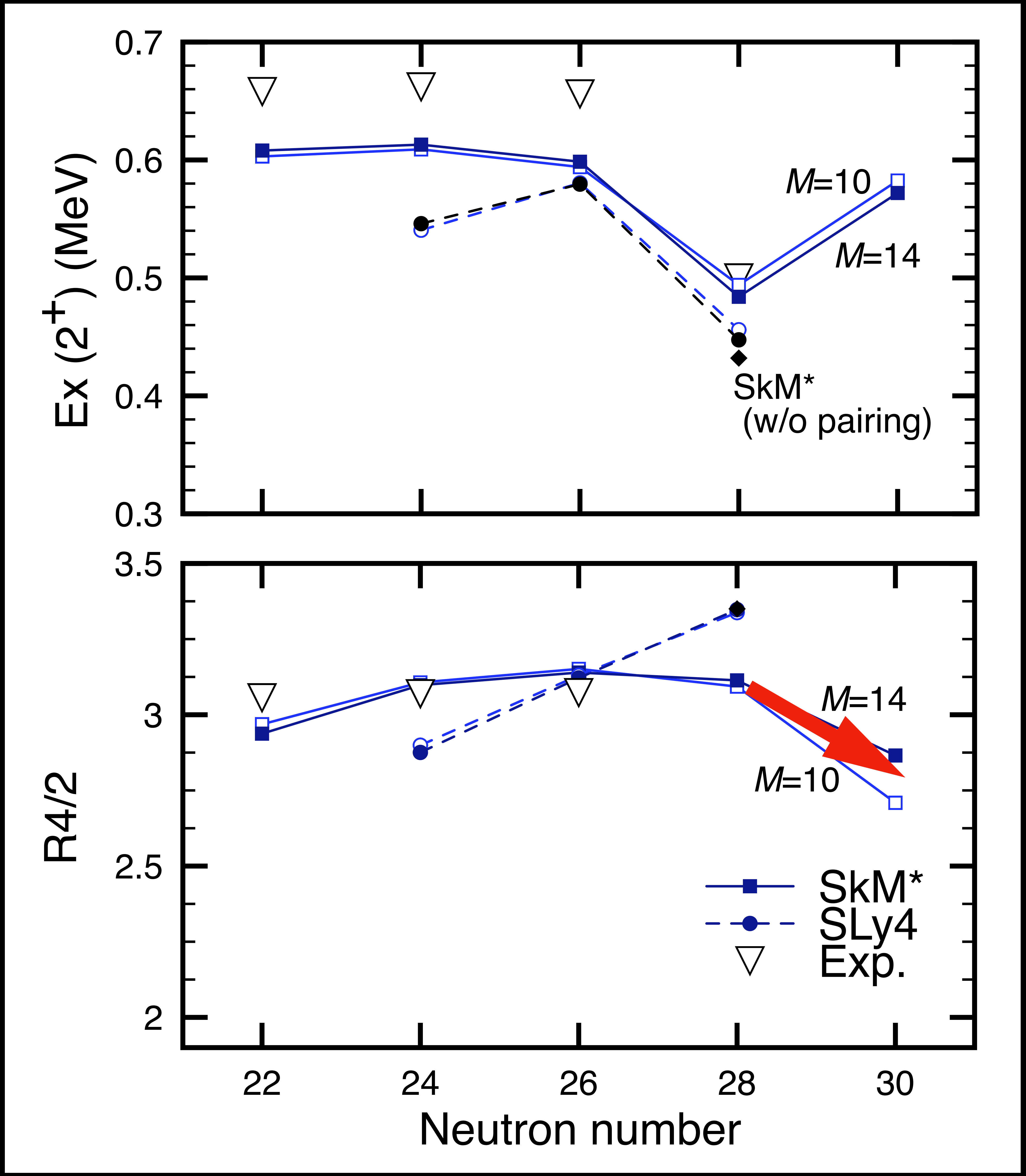


both SkM* and SLy4

reproduce the lowering of $E(2_1^+)$ in $^{40}$Mg

predict different $R_{4/2}$ values

SLy4 + YSN pairing

both neutrons and protons are unpaired

similar result using SkM* w/o pairing

experimental $R_{4/2}$ determines the normal/superfluidity of $^{40}$Mg

# Evolution of triaxial deformation in $^{42}$Mg

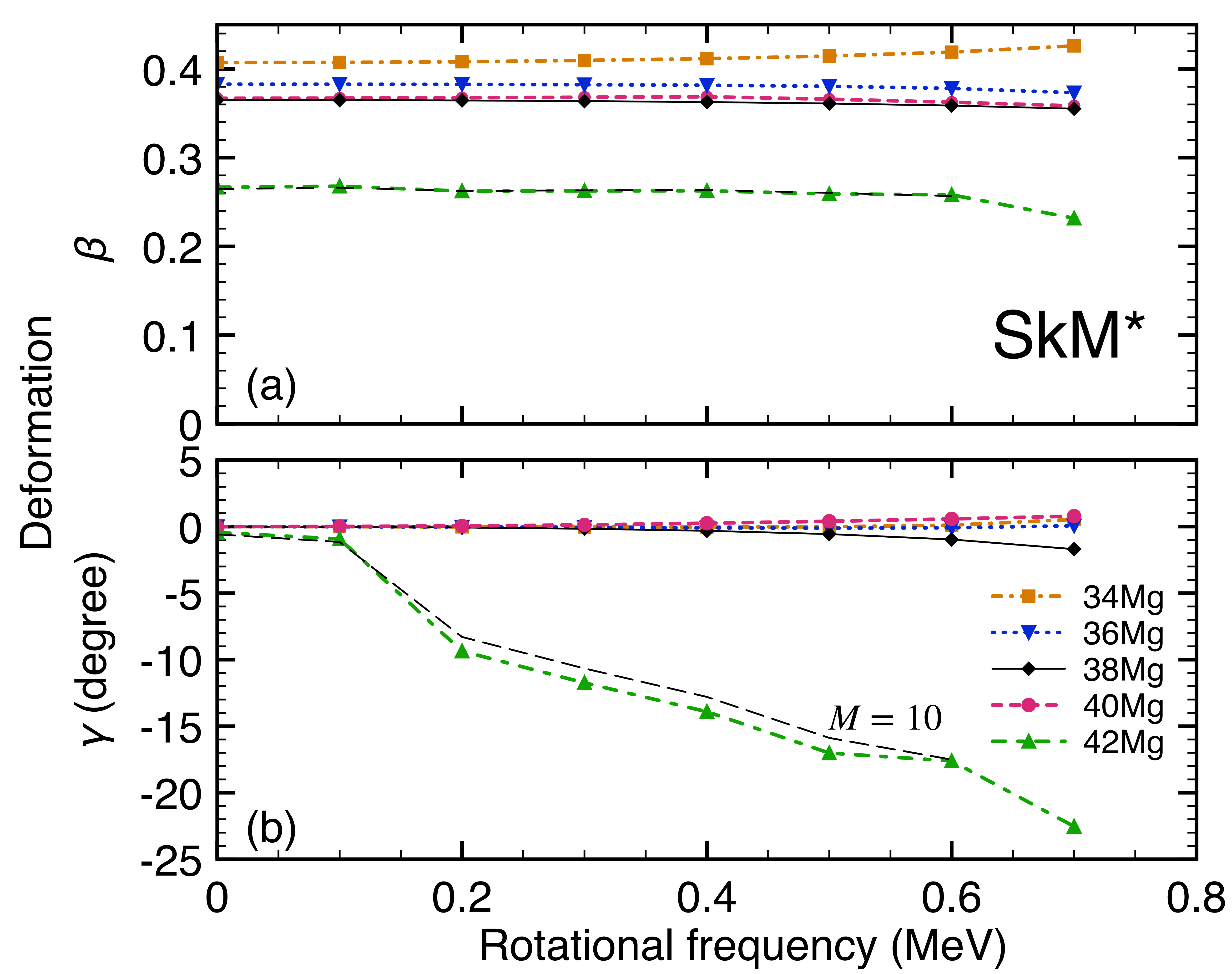


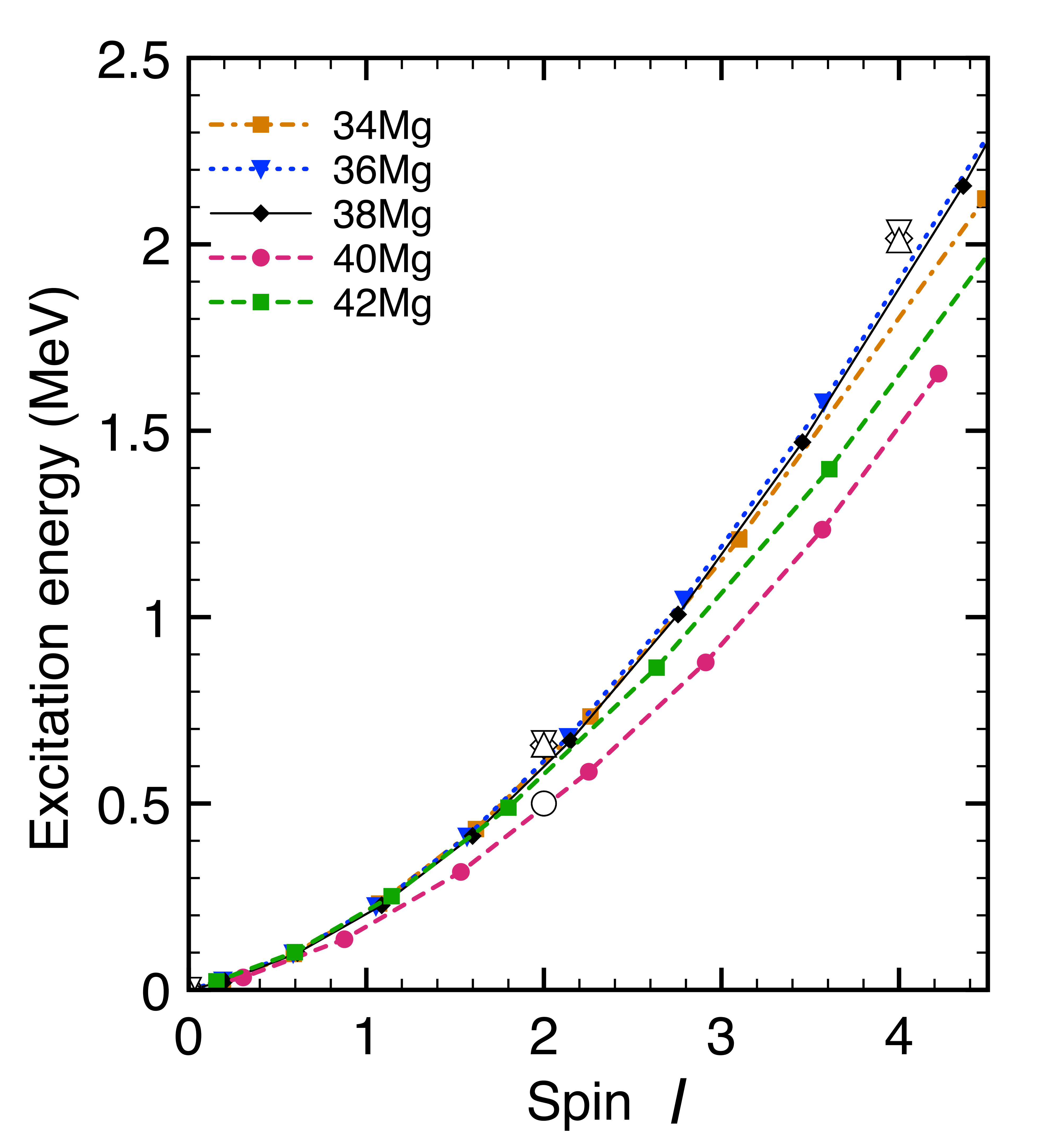


def. parameters for protons

$$J_z^2 = I(I+1)$$

## Summary

first cal. of the cranked-Skyrme–Kohn–Sham–Bogoliubov in 3D mesh

practical/reasonable in investigating the interplay among deformation, pairing, and continuum

neutron-rich Mg isotopes near the drip line

**anomaly in $^{40}$Mg**

unlikely due to the weak binding

suppression/vanishing of pairing of neutrons

discriminated by the $R_{4/2}$ value

**triaxial dynamics in $^{42}$Mg**

weak-binding effects visible: neutrons rms radius, triaxial def., $R_{4/2}$

# Quasineutron Routhians in $^{34}Mg$

## Mixed-type

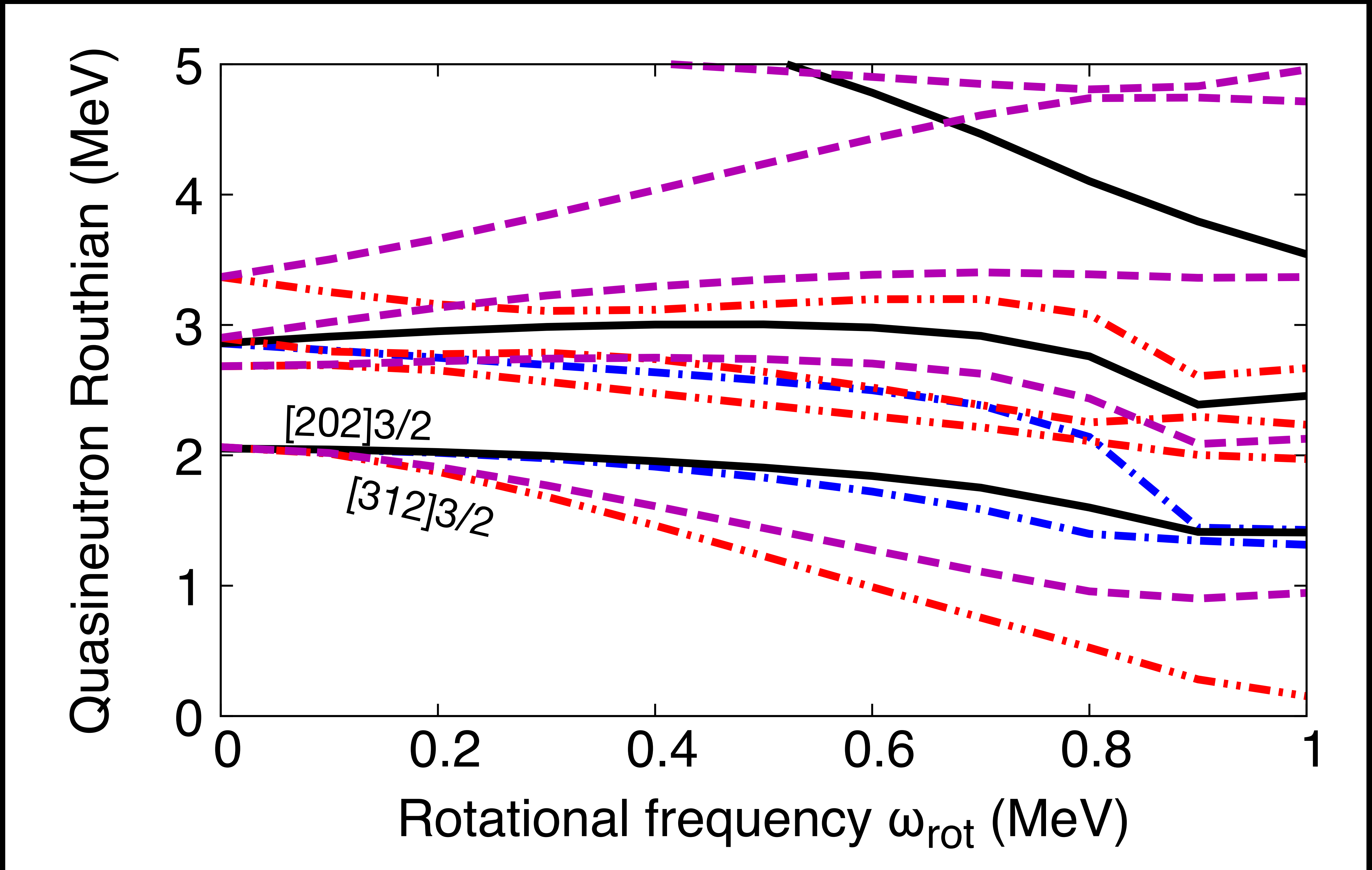


## Volume-type

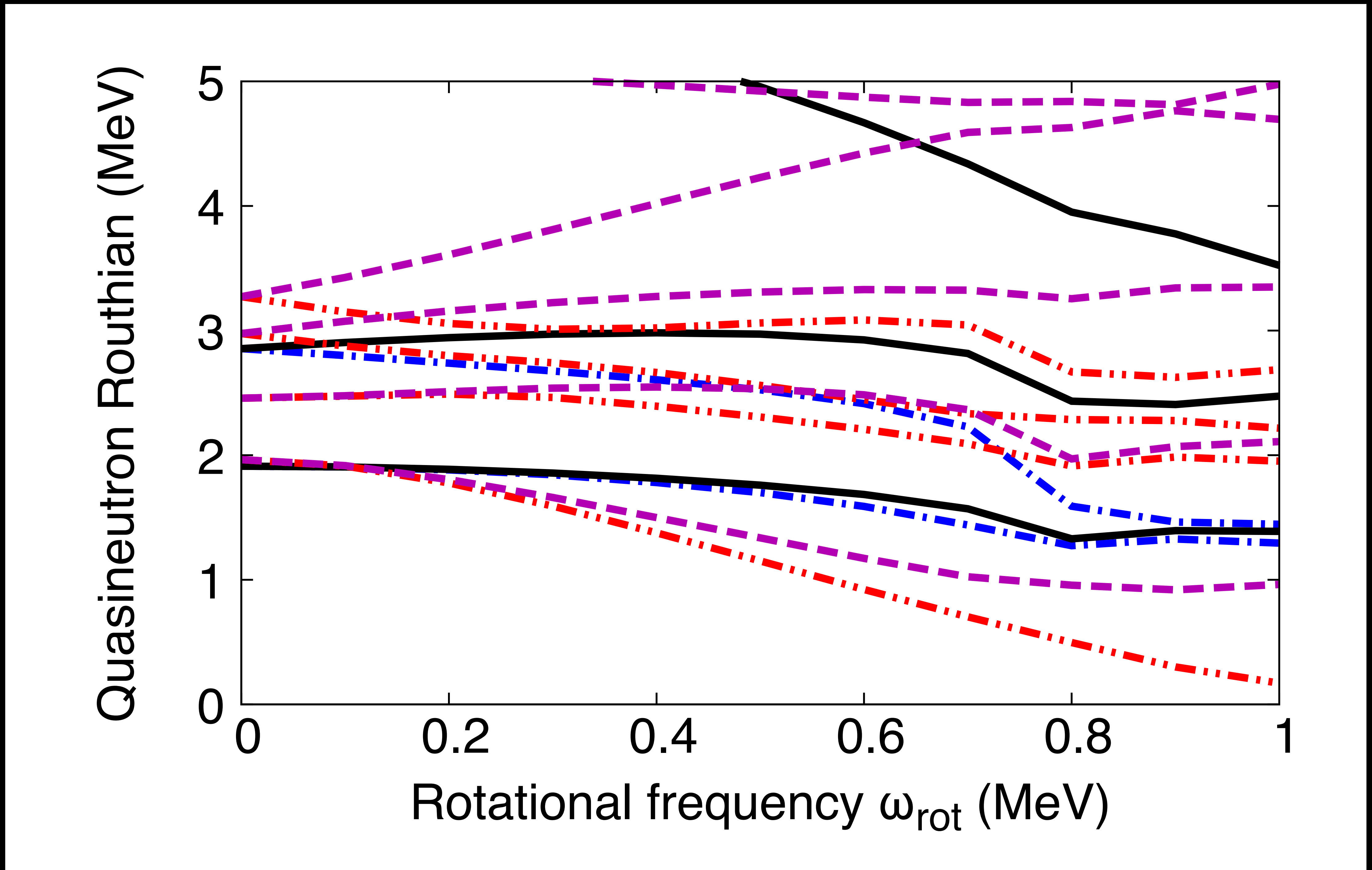

# Ground-state properties

SkM* + YSN pairing

| | $^{34}$Mg | $^{36}$Mg | $^{38}$Mg | $^{40}$Mg | $^{42}$Mg |
|---|---|---|---|---|---|
| $\lambda_n$ | -4.08 | -3.19 | -2.42 | -1.62 | -1.15 |
| $\lambda_p$ | -18.7 | -20.1 | -22.3 | -23.8 | -25.5 |
| $\sqrt{\langle r^2 \rangle_n}$ | 3.51 | 3.59 | 3.67 | 3.78 | 3.83 |
| $\sqrt{\langle r^2 \rangle_p}$ | 3.14 | 3.16 | 3.18 | 3.21 | 3.19 |
| $\beta_n$ | 0.35 | 0.31 | 0.28 | 0.29 | 0.18 |
| $\beta_p$ | 0.41 | 0.38 | 0.37 | 0.37 | 0.27 |

# Ground-state properties: density distribution of neutrons

34Mg

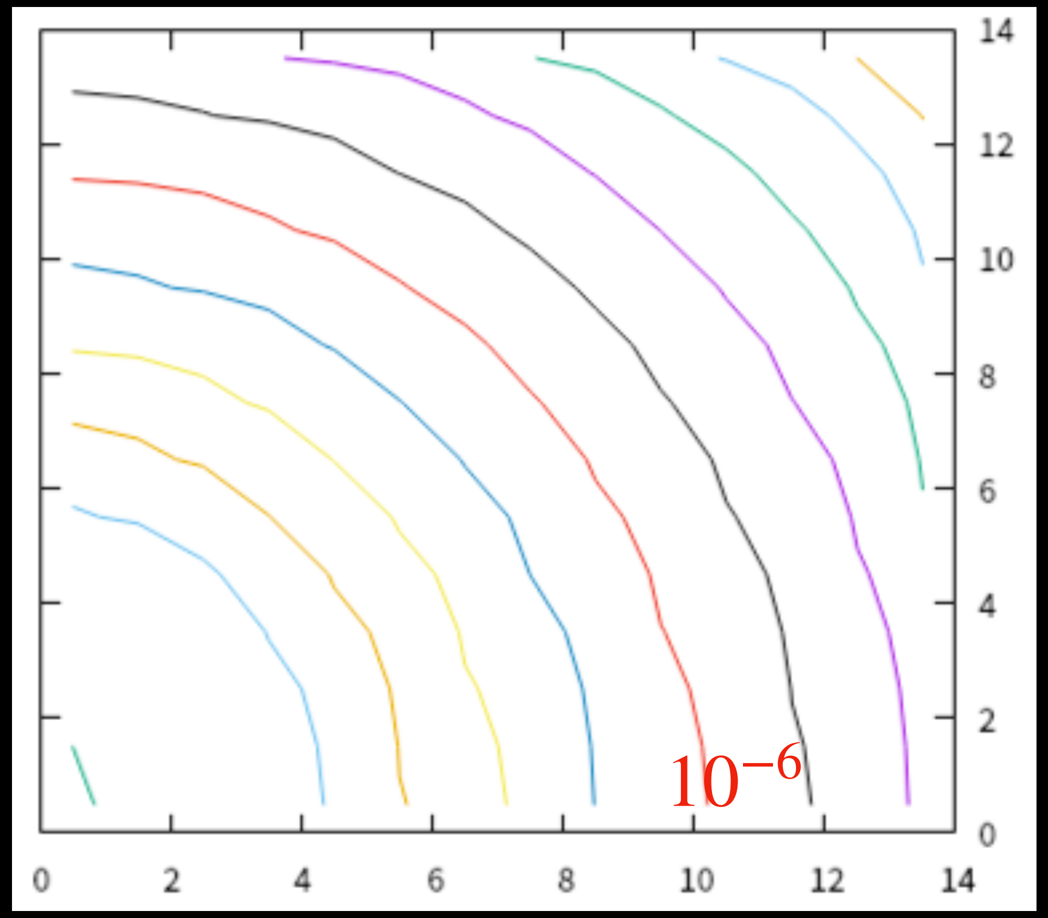


36Mg

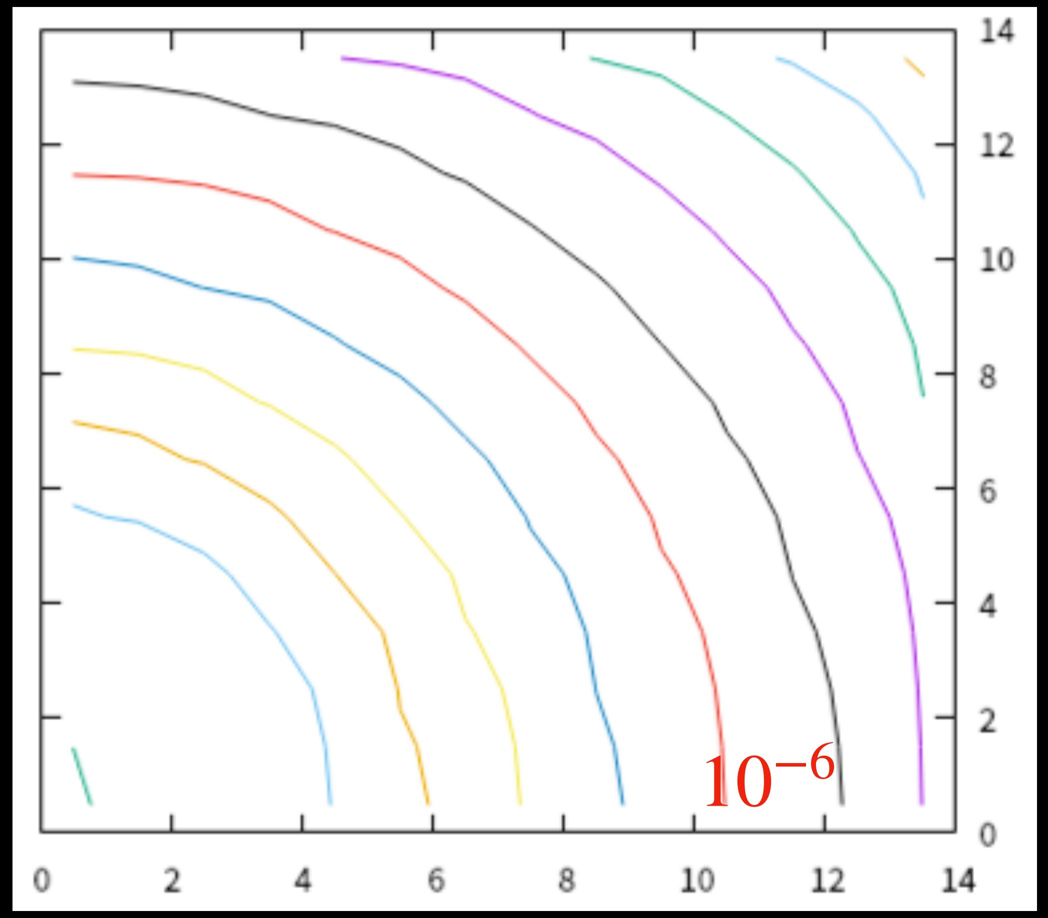


Nakada–Takayama, PRC98(2018)011301

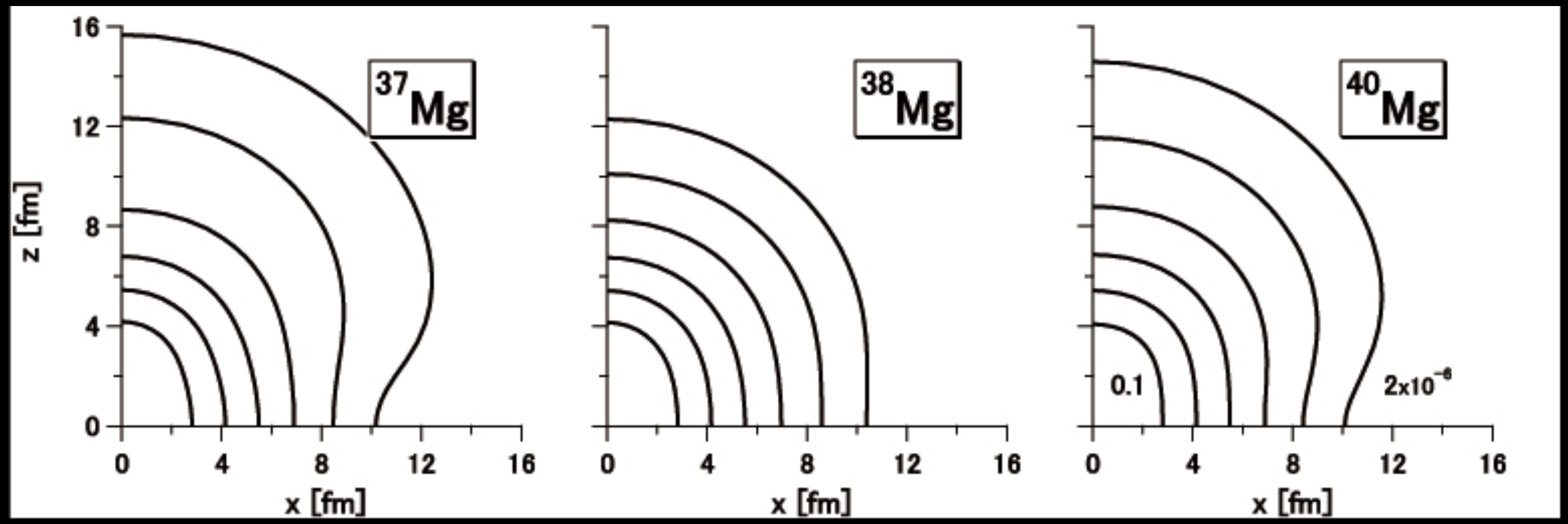


38Mg

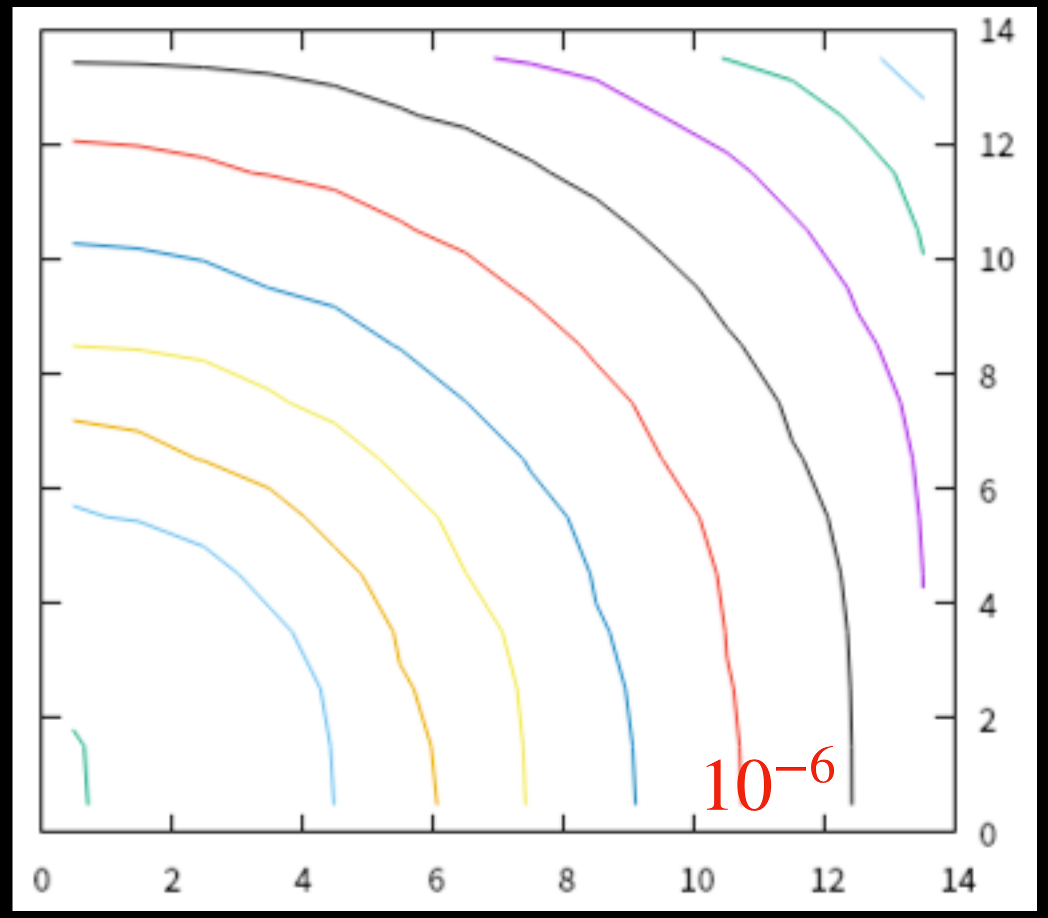


40Mg

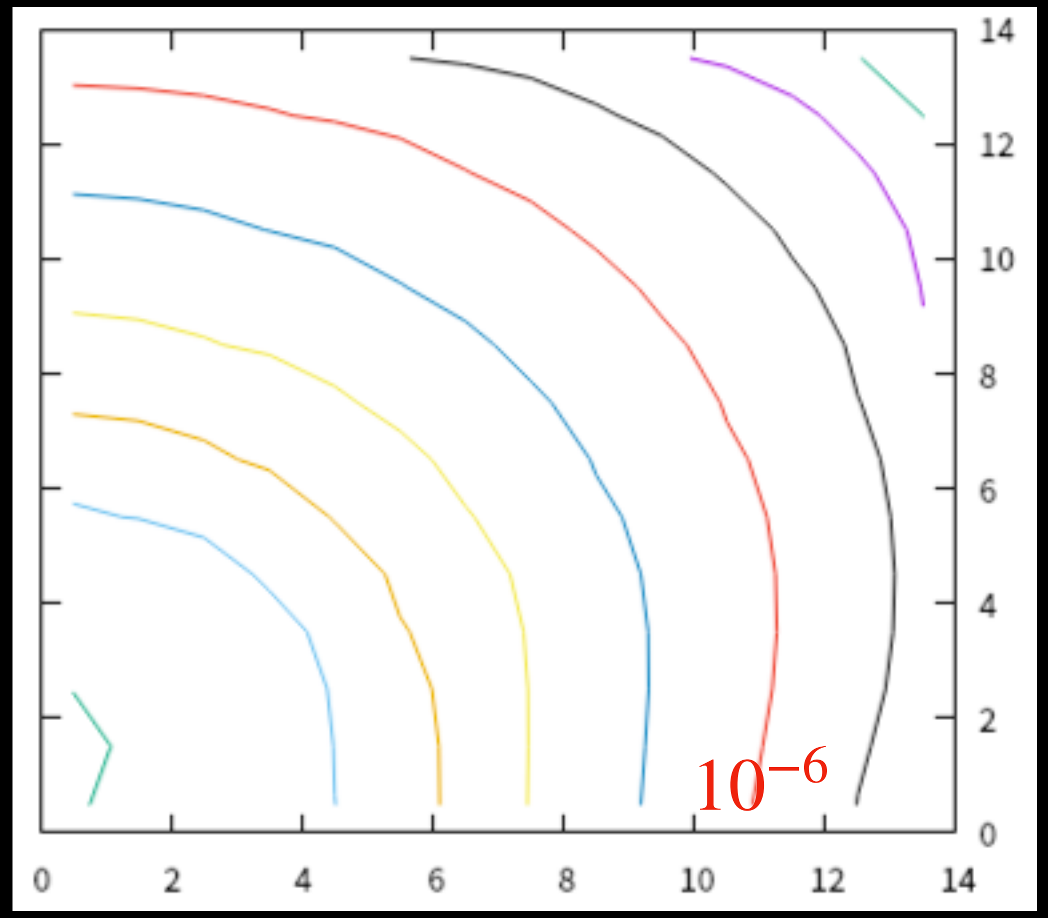


42Mg

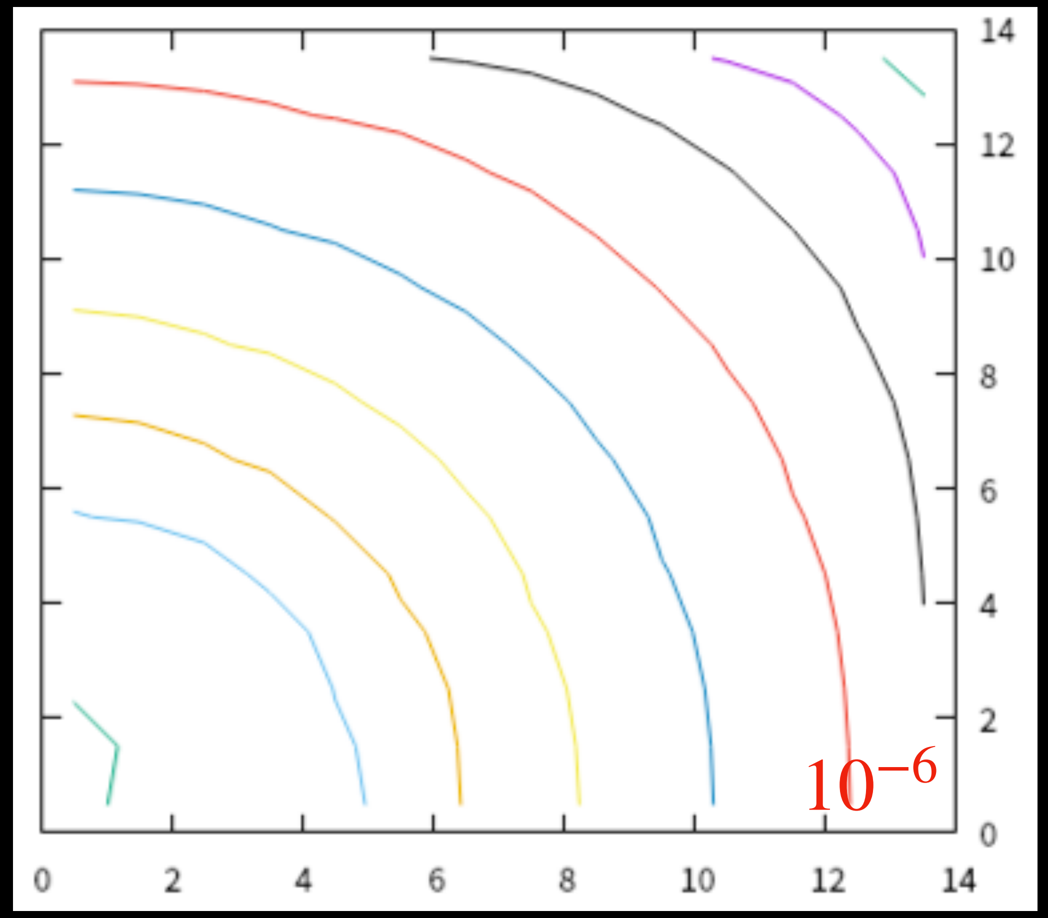

40Mg

SkM*+mixed

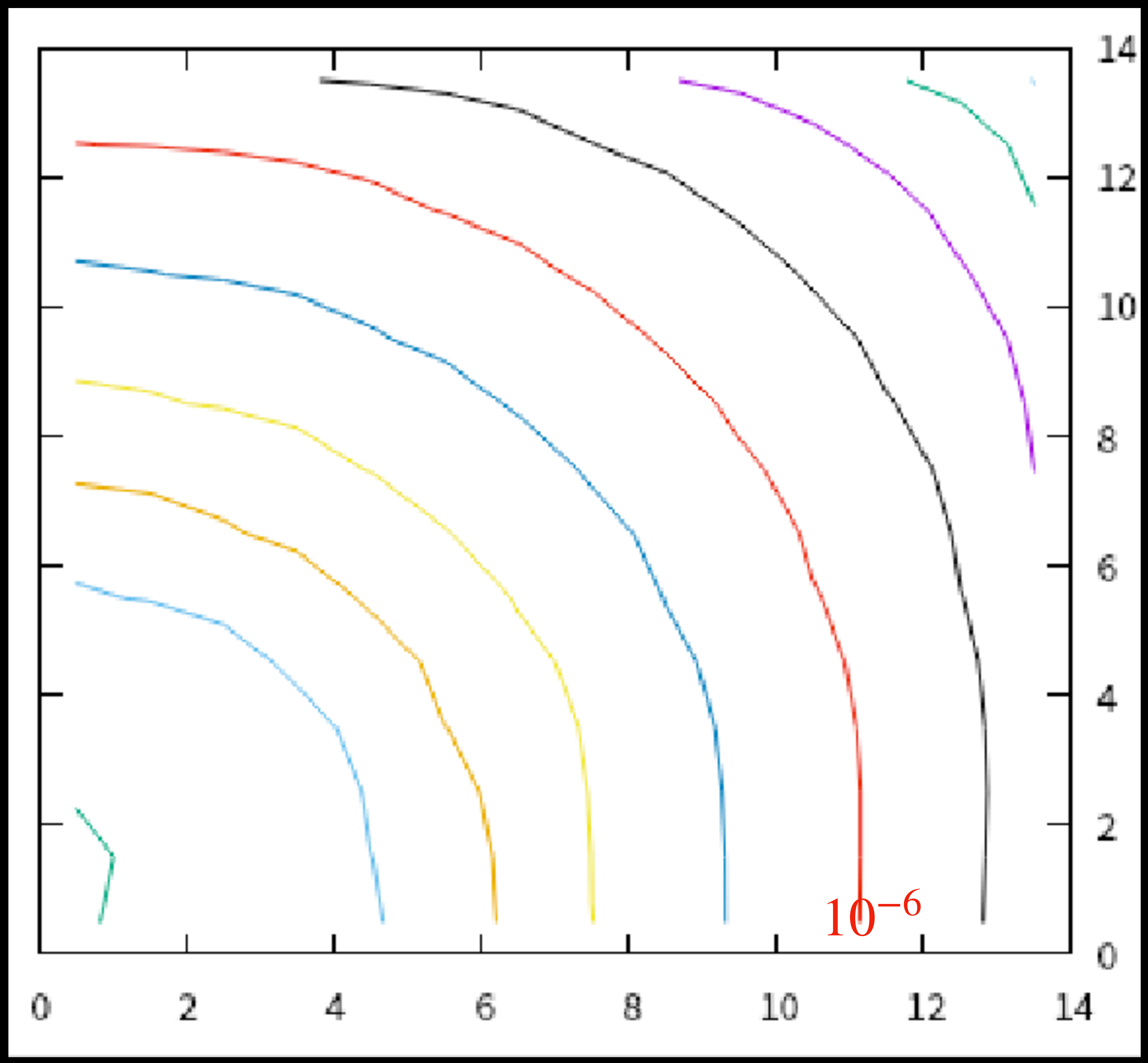


$\Delta_n = 1.6$ MeV

SkM*+YSN

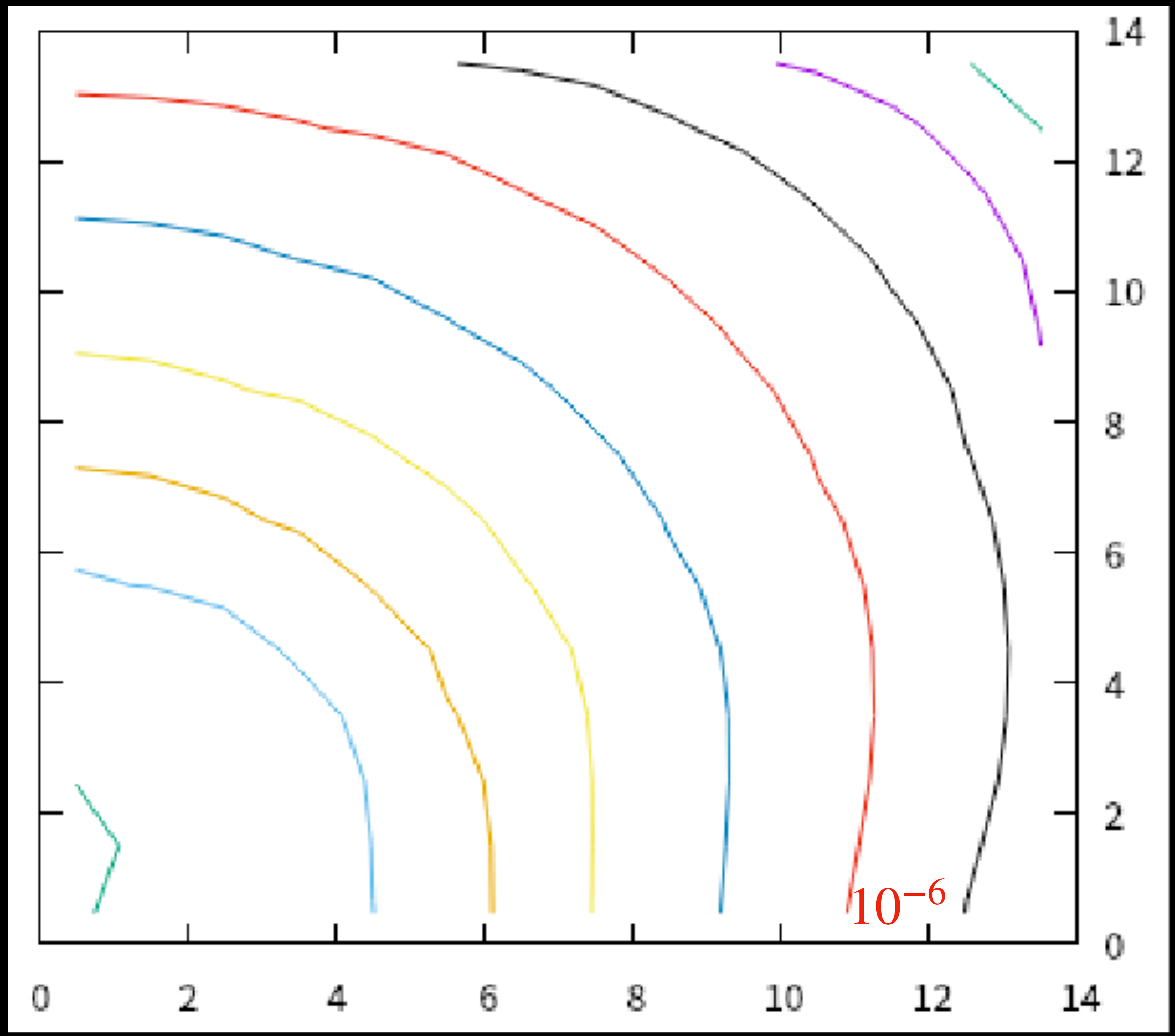


$\Delta_n = 0.5$ MeV

SkM* w/o pairing

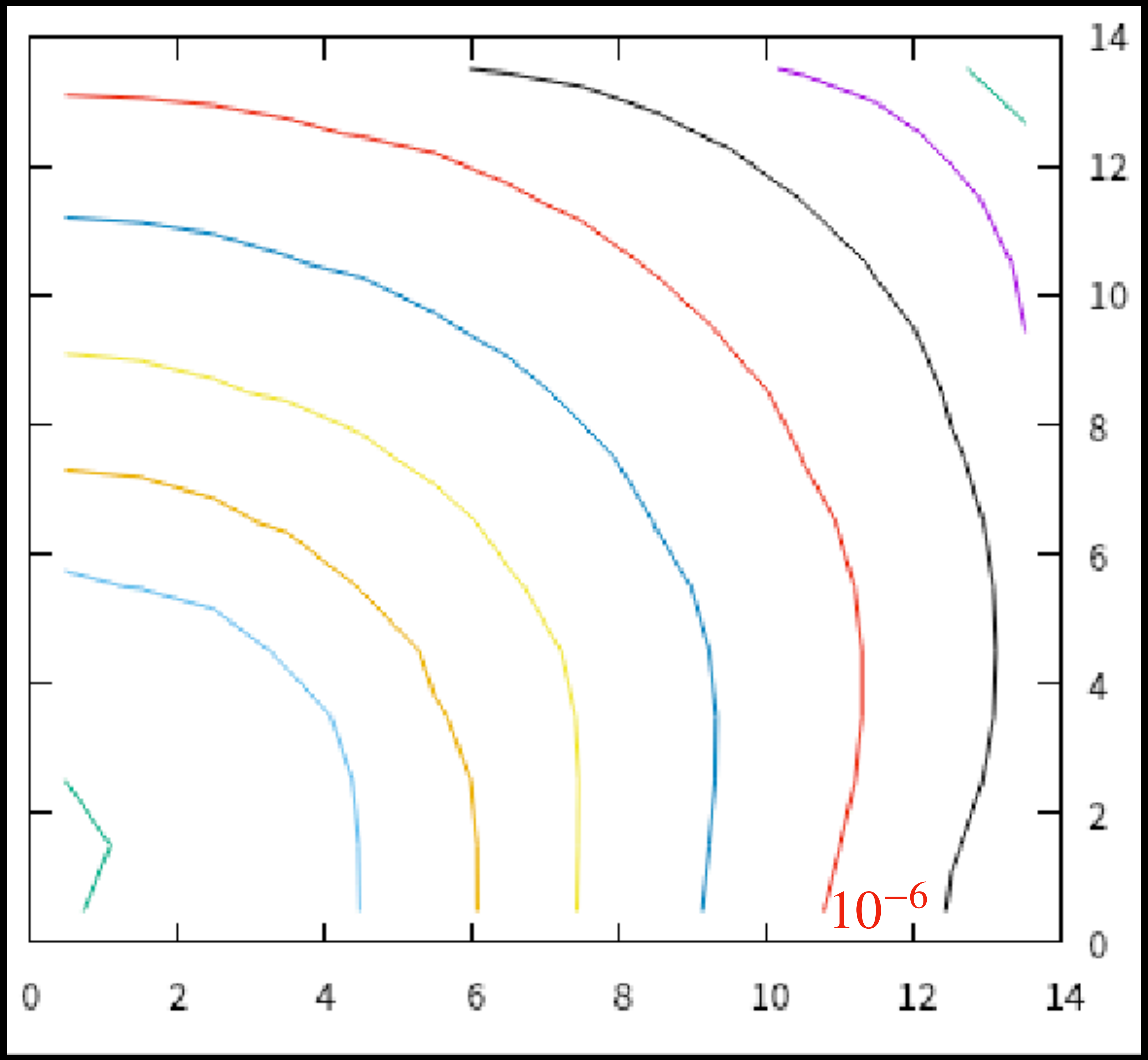


| | SkM*+mixed | SkM*+YSN | SkM* w/o pairing |
|---|---|---|---|
| Total BE: | -282.06 MeV | -281.10 MeV | -281.05 MeV |
| pairing E: | -10.4 MeV | -1.38 MeV | |
| $\lambda_n$ : | -1.61 MeV | -1.62 MeV | |

SkM*+YSN

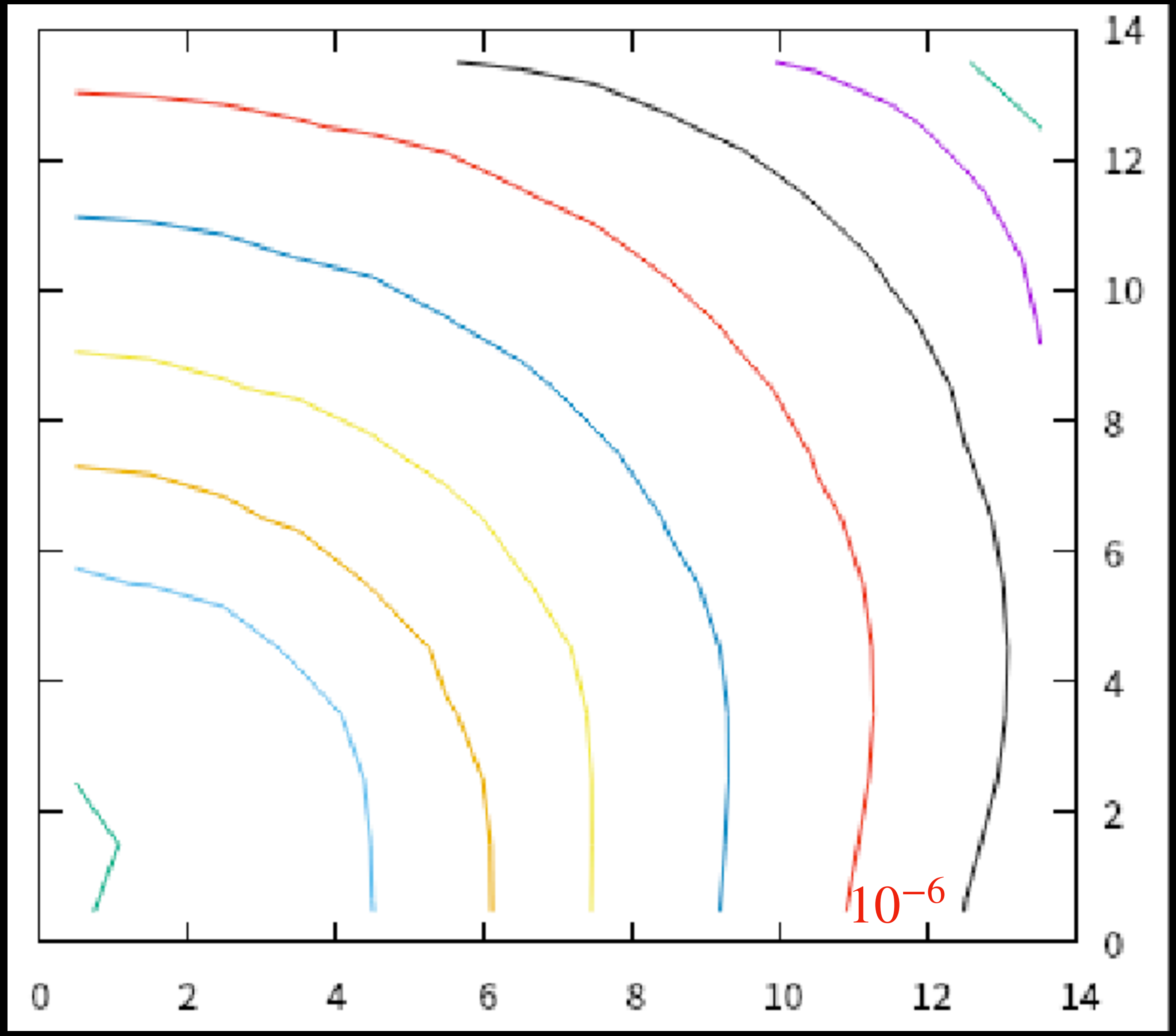


$\Delta_n = 0.54$ MeV

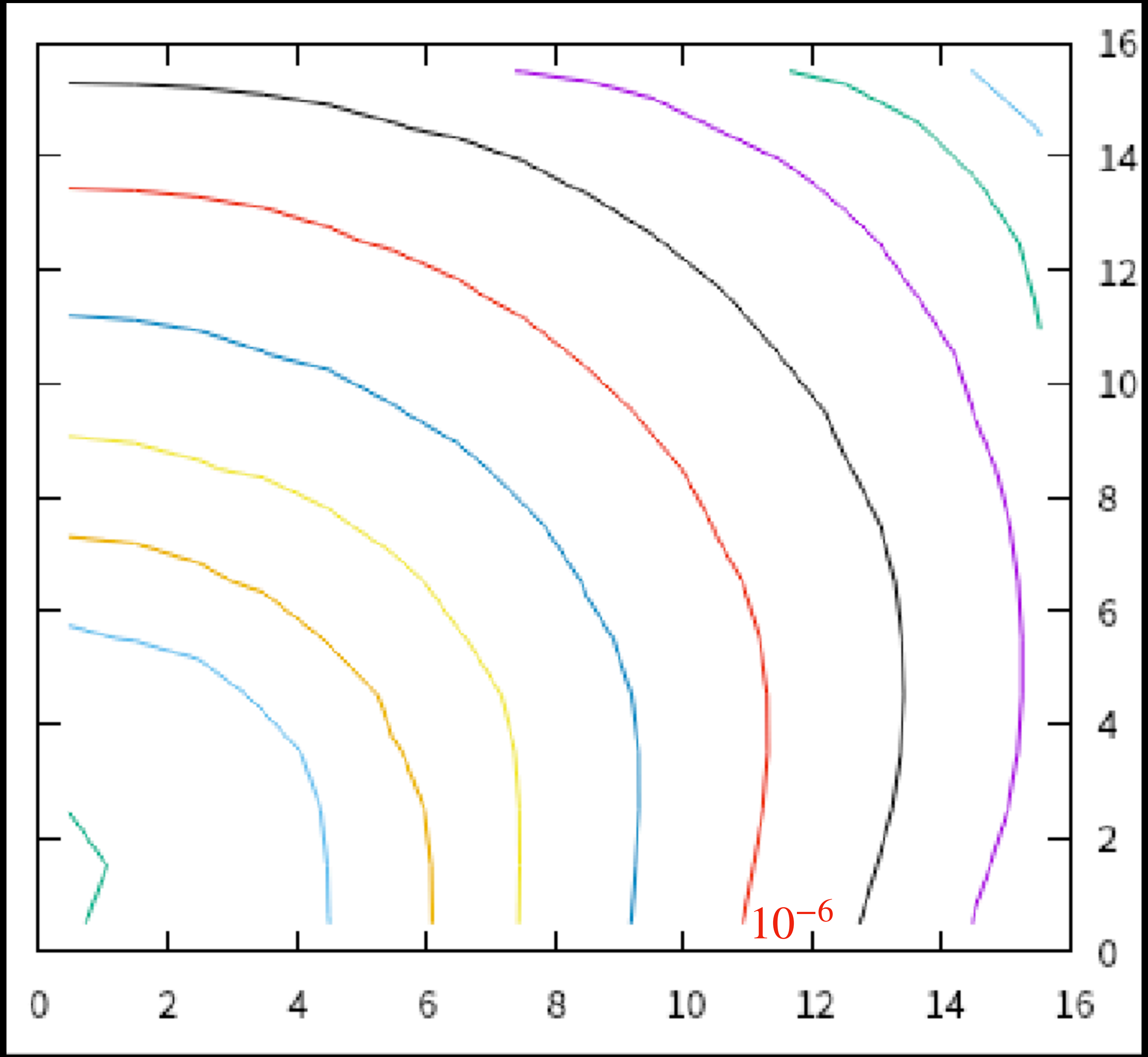


$\Delta_n = 0.52$ MeV

| | | |
|---|---|---|
| Total BE: | -281.10 MeV | -281.10 MeV |
| pairing E: | -1.38 MeV | -1.37 MeV |
| $\lambda_n$ : | -1.62 MeV | -1.63 MeV |

SLy4 w/o pairing

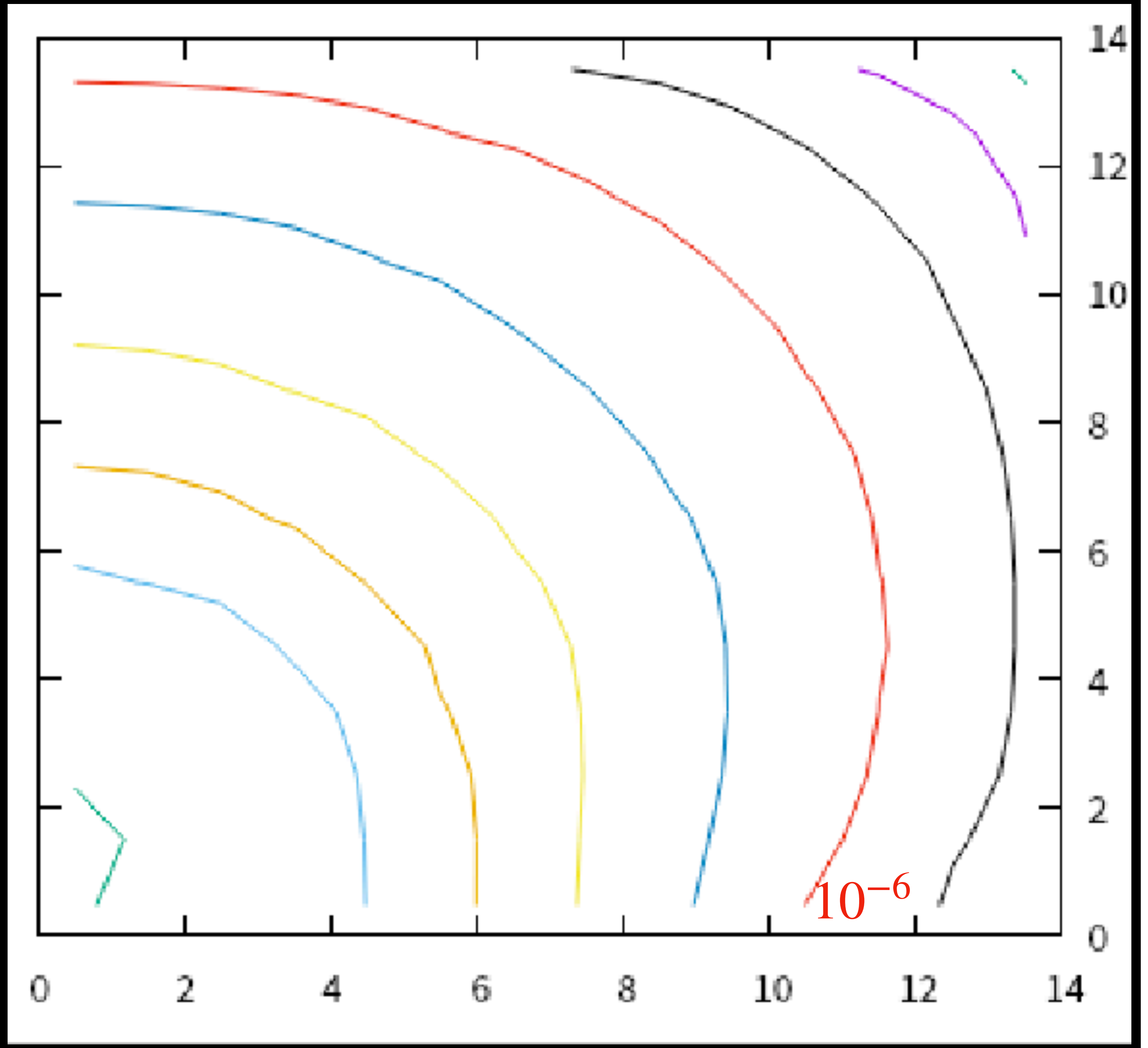


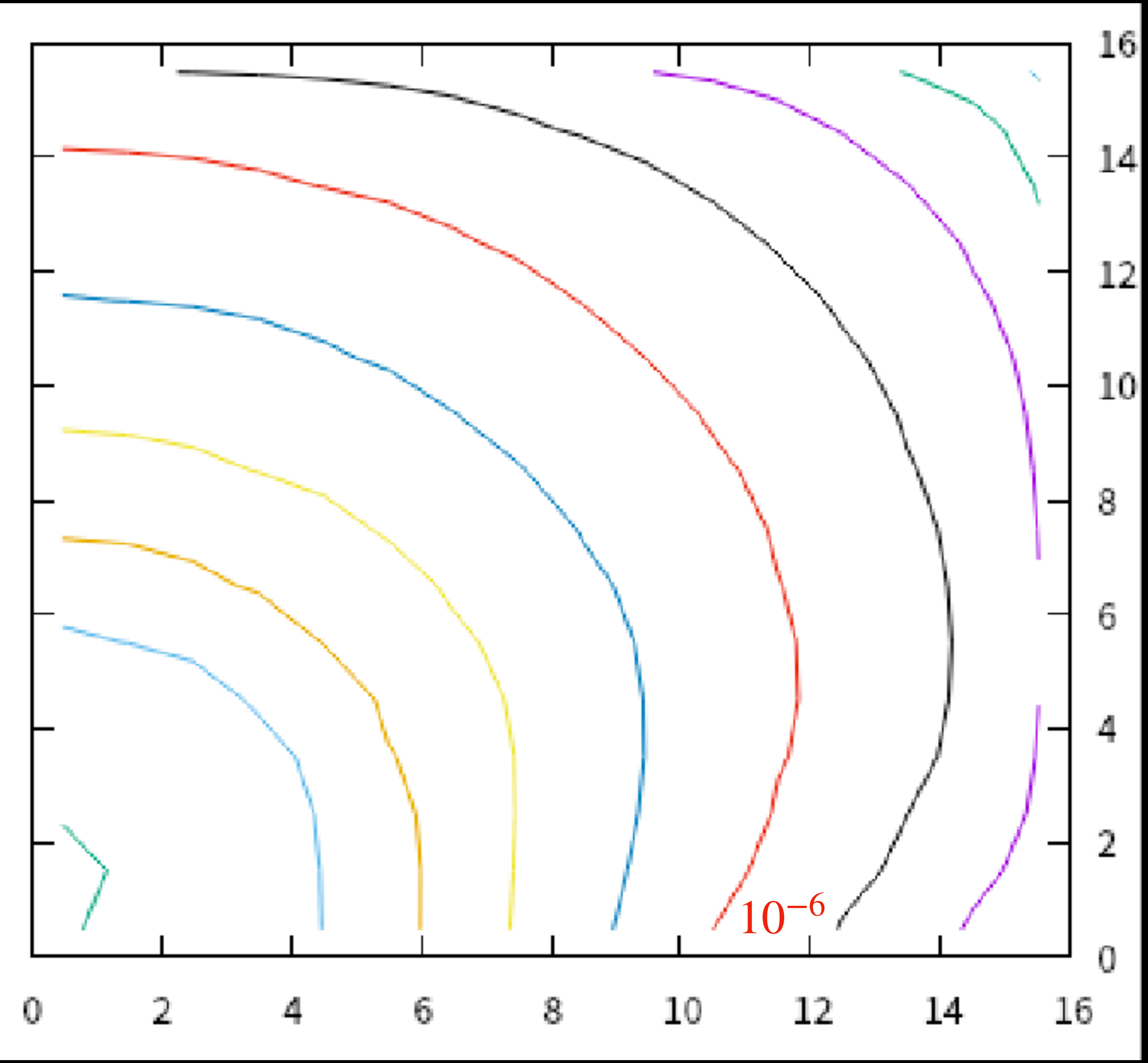


Total BE: -270.22 MeV -270.22 MeV